STUDY OF THE OPTICAL AND AC ELECTRICAL PROPERTIES OF PLASMA POLYMERIZED BENZONITRILE THIN FILMS

By

Salma Akter

Roll No. 100714020F

Session: April, 2008

A dissertation submitted to the Department of Physics, Bangladesh University of Engineering and Technology (BUET) in partial fulfillment of the requirement for the degree of

MASTER OF PHILOSOPHY (M.Phil.) in Physics

Department of Physics

Bangladesh University of Engineering and Technology (BUET),

Dhaka-1000, Bangladesh.

Feb, 2014

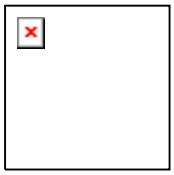

BUET

CANDIDATE'S DECLARATION

It is hereby declared that this thesis or any part of it has not been submitted elsewhere for the award of any degree or diploma.

Dedicated to

My beloved **Parents**, **Uncle** and dear **Husband**

Who inspired and influenced me for higher study

T A B L E O F C O N T E N T S

List of Figures

List of Tables

Glossary

ABS	Absorbance
ac	Alternating Current
Al	Aluminum
BN	Benzonitrile
CBD	Chemical Bath Deposition
cc	Capacitively Coupled
CRT	Cathode-ray tube
d	Sample Thickness
dC	Direct Current
DEA	2, 6 Diethylaniline
DSC	Differential Scanning Calorimetry
DTA	Differential Thermal Analysis
E_{gd}	Direct transition energy gap,
E_{gi}	indirect transition energy gap,
FL	Fermi Level
FTIR	Fourier Transform Infrared
I	Current
I	Intensity of Radiation
IR	Infrared
k	Boltzmann Constant
k	Extinction Co-efficient
MHz	Mega Hertz
PECVD	Plasma Enhanced Chemical Vapor Deposition
PPBN	Plasma Polymerized Benzonitrile
PPDEA	Plasma Polymerized 2, 6 Diethylaniline
PPDP	Plasma-polymerized Dipheny1
PPm-X	Plasma-Polymerized m-Xylene
PPPA	Plasma-Polymerized Polyaniline
PVD	Physical Vapour Deposition

rf	Radio Frequency
SCLC	Space Charge Limited Conduction
SEM	Scanning Electron Microscopy
T_g	Glass Transition Temperature
T_m	Melting Point
TGA	Thermo Gravimetric Analysis
TSDC	Thermally Stimulated Depolarization Current
UV-vis	Utraviolet-Visible
V	Voltage
XPS	X-ray Photoelectron Spectroscopy
α	Absorption Coefficient
β_{exp}	Experimental β Co-efficient
β_S	Schottky Co-efficient
β_{PF}	Poole-Frenkel Co-efficient
ϕ	Columbic barrier height of the electrode polymer interface
ϕ_c	Ionization potential of the PF centers
λ	Wavelength
ΔE	Activation Energy
σ_{ac}	ac Electrical Conductivity
ε	Dielectric Constant
ε_0	Permittivity of Free Space
μ	Mobility of Charge Carrier

A C K N O W L E D G E M E N T S

At the very first, I express my satisfaction to praise the almighty Allah who has given me the strength and opportunity to complete my thesis work with success.

It is my privilege to offer my heartiest gratitude and profound respect to Prof. Dr. Md. Abu Hashan Bhuiyan, Department of Physics, Bangladesh University of Engineering Technology (BUET), for providing the opportunity to work in such a dynamic field of research. I am indebebted to him for his continuous guidance, suggestions and kind supervision throughout the research work and also for acquainting me with the advance research.

I am thankful to the authority of BUET for giving me necessary permission along with the financial support and ensuring the opportunity to access all sorts of facilities to complete this research work successfully.

I am grateful to my respected teacher Prof. Dr. Afia Begum Head, Department of Physics, for allowing me to work in this Department and for her valuable suggestions regarding my thesis. I am obliged to Prof. (Rtd) Dr. Mominul Huq, Prof. (Rtd) Dr. Nazma Zaman(Rtd), Prof. Dr. Jiban Podder, Prof. Dr. Md. Feroz Alam Khan, Prof. Dr. Md. A K .M. A. Hossain, Prof. Dr. Md. Mostak Hossain and Dr. Md. Forhad Mina, Associate Professor of the Department of Physics, BUET for their inspiration, affection and constructive suggestions for this advanced research work. I am also thankful all other teachers of the Department for giving inspiration during the work.

I would like to take the opportunity to express my appreciation to Dr. Rummana Matin for her dedicated support preparing thesis successfully by allowing her precious time for me. I am also thankful to Dr. Sunirmal Majumder and Dr. Rama Bijoy Sarker, for their cooperation, affection and inspiration throughout the work.

I would like to thank Mr. Harinarayan Das, Scientific Officer, AECD and thankful to Ms. Happy Dey. I would like to thank Dr. M.A. Gafur Senior Scientific Officer, Pilot Plant & Process Development Center of Bangladesh Council for Scientific & Industrial Research (BCSIR) and the authority of BCSIR, Dhaka, for allowing me to use the available facilities in that laboratory.

I am also thankful to all the staff members Mr. Md. Idris Munshi, Mr. Md. Liaquat Ali, Mr. Md. Nurul Haque, Mr. Md. Lutfor Rahman Sarker, Mr. Swapan Kumar Das, Mr. Md. Mozammel Haque, Mr. Md. Abu Taher and Mr. Md. Lutfor Rahman, Department of Physics, BUET for their sincere help.

Finally, I would like to express my gratitude to my beloved dear husband and all other family members for their multifaceted support throughout the journey to reach the place which I am occupy now.

Salma Akter

Abstract

Plasma polymerization technique was applied to deposit plasma polymerized benzonitrile (PPBN) thin films from benzonitrile(BN) monomer at room temperature by a parallel plate capacitively coupled glow discharge reactor. It is seen from the FTIR spectrum of the PPBN thin films that the peak at 1595 cm^{-1} for C=N stretching is observed in lower intensity than that is observed in BN. The peaks for aromatic C=C bands at 1560 and 1455 cm^{-1} are retained in PPBN. The C-C=N deformation vibration at 545 cm^{-1} was also observed in PPBN spectrum, indicating that a certain amount of C≡N bonds remained unreacted. These observations indicate that plasma polymerization technique has modified the basic structure of the monomer. The thermal analyses suggest that the thermal stability temperature, Ts of BN and PPBN is about 378 and 500 K respectively. The values of E_{gd} vary from 2.80 to 2.47 eV, and those of E_{gi} vary from 2.20 to 1.73 eV as the thickness vary from 233 to 352 nm for PPBN thin films. From the Ultraviolet visible spectroscopic analyses it is reveled that as the thickness of the films increases, some fragmentation/crosslinking may develop within the bulk of the material with increasing deposition time and as a consequence lower energy gaps are observed. The decrease in E_g with increasing thickness is assumed to appear due to the merge of defect states and generation of sublevels at the end of the valance band and conduction band.

AC conductivity, σ_{ac}, increases as the frequency increases. The frequency exponent, *n* of PPBN thin films correspond to Debye-type in the lower frequency region and in the high frequency region correspond to the relaxation process other than Debye type. The value of the ac activation energy and the increase of $\sigma_{ac}(\omega)$, with the increase of frequency confirms that hopping conduction is the dominant current transport mechanism in PPBN films. The dielectric constant (ε') decreases slowly with increasing frequency and the values of ε' lie between 9 and 24 at different temperatures in the low frequency region (<10 kHz). The loss tangent is found to increase with the increase in frequency having a loss peak around 10^5 Hz.

CHAPTER 1

GENERAL INTRODUCTION

CHAPTER 2

THEORETICAL BACKGROUND

CHAPTER 3

EXPERIMENTAL DETAILS

CHAPTER 4

RESULTS AND DISCUSSION

CHAPTER 5

CONCLUSIONS

1.1 Introduction

The tendency to make dream into reality and physical involvement to develope an advanced living culture is to some extent entertained by plasma polymeric materials, which of opened up a new era in the field of surface coating, electronic, microelectronic, photoelectronic, biomedical membrane separation and biosensors due to their sustainable thermal, structural optical electrical properties [1]. The films obtained by plasma polymerization are generally of high quality, homogeneous, adherent, thermally stable and pinhole free [2-4].

In a number of applications, both conductivity and transparency are required, for which metals, inorganic conductors and conducting polymers can be used. In strive for reduction in size, costs and weight of electronic equipment, the combination of polymeric properties and conductivity would be highly advantageous. This has long been recognized by the scientific and industrial community and has resulted in extensive research in this field.

Organic materials have been the subject of intense scientific investigation for the past 50 years .Due to often weak bonding between organic molecules in the solid state, they share many of the properties of both semiconductors and insulators, and hence their study has led to a deepening of fundamental understanding of the electronic and optical properties of polymers. Thin films of these organic materials have received a great deal of interest due to their extensive applications in the fields of mechanics, electronics and optics [5-6].

Now a days, material preparation, processing and surface modification becomes prominent area of research in the development of science and technology. Among different kinds of polymerization techniques, plasma polymerization emerges as a most important technique for the preparation of organic thin films .Plasma polymerization is an attractive technique, using which it is possible to deposit thin films from any monomer onto variety of substrate materials. Furthermore, it is a solvent- free, fast and versatile process. [7-10].

Study on different plasma polymerized organic polymer is being carried out in the Solid State Laboratory of Bangladesh University of Engineering and Technology over the past few years. It is seen that the plasma polymerization emerges as a very important technique for thin film deposition and surface modification. So in the present

research work, plasma polymerization technique has been used for the preparation of thin films. On reviewing the earlier works, it is seen that not much work has been done on the thin films prepared using Benzonitrile (BN) by plasma polymerization technique. That's why this monomer has been chosen for the polymerization and to investigate the physical properties of the thin film. This type of material is used as coatings, insulators, dielectrics, electronic, optoelectronic, etc. That is why this material was chosen as a potential organic monomer for thin film preparation.

1.2 Review of Earlier Research Work

Polymer science is one of the fields which have to a great extent contributed to the affluent of human civilization. For the enlargement of science and technology the active role of polymer is predictable. Due to their large application polymers, plasma polymerization technique become very popular now a days. A large number of

Researches all over the world in the nook and corner are searching for new invention in this field and finding, are publishing in national and international journals. The recent development of science and technology of thin films organic compounds produced by plasma polymerization has drawn much attention of the scientist to investigate their various properties. The attention in plasma-polymerized thin films as a possible dielectric material has triggered academic interest in the polymerization process [11].

Work in this field has inspired several investigators to characterize the thin film polymers produced from organic monomers by polymerization process.

The structural behavior of plasma polymerized thin films is different than that of the conventionally prepared polymer thin films. Fourier transformed infrared (FTIR) spectroscopic analysis; X-ray photoelectron spectroscopy (XPS), elemental analysis (EA), etc. provide information about the chemical structure of the plasma polymers. Ultraviolet-Visible (UV-Vis) spectroscopic analyses of organic or inorganic materials can provide the information about electronic structure and can be ascertained the existence of optical transition mechanisms: allowed direct and indirect transitions.

Majumder and Bhuiyan [12] employed electrical glow discharge technique for the preparation of plasma polymerized vinylene carbonate (PPVC) thin films of aluminum/thin film/aluminum sandwich structure at room temperature by a parallel

plate capacitively coupled reactor. The structural investigation of the monomer VC and PPVC was performed by FTIR. They found Ohmic current conduction in the low voltage region and non Ohmic conduction in the high voltage region and the most probable conduction mechanism in the PPVC thin films is of Schottky type. Plasma polymerized 1, 1, 3, 3-tetramethoxy-propane thin films of different thicknesses were prepared by

Afroze and Bhuiyan [13] prepared 1, 1, 3, 3-tetramethoxypropane thin films through glow discharge plasma polymerization technique. They found smooth, uniform and pinhole free films with aliphatic conjugation of C=C and C=O bonds. There was formation of C-O-C bond owing to rearrangement of oxygen due to heat treatment of PPTMP thin films. The allowed direct transition and indirect transition (Egi) energy gaps were found to be about 2.92 to 3.16 eV and 0.80 to 1.53 eV respectively, for as deposited PTMP samples of different thicknesses. The Eqi of two samples of different thicknesses heat treated at 673 K for 1 hour are 0.55 and 0.65 eV.

Plasma polymerized tetraethylorthosilicate (PPTEOS) thin films were deposited by Zaman and Bhuiyan [14] on to glass substrates at room temperature by a parallel plate capacitively coupled glow discharge reactor. The conduction in PPTEOS is dominated by hopping of carriers between the localized states at the low temperature and thermally excited carriers from energy levels within the band gap in the vicinity of high temperature.

Chowdhury and Bhuiyan [15, 16] investigated the optical and electrical properties of plasma polymerized biphenyl (PPDP) thin films. They was concluded that the band gap was not affected appreciably by heat treatment whereas it was modified on aging. The ac conductivity was more dependent on temperature in the low frequency region than in the high frequency region. Dielectric constant is dependent on frequency above 303 and 343 K in the as deposited and heat treated PPDP respectively. The dielectric data analysis shows the existence of distribution of relaxation time in these materials

Matin and Bhuiyan [17] revealed by Fourier transform infrared spectroscopic analyses of 2, 6 diethylaniline monomer and plasma polymerized 2, 6 diethylaniline (PPDEA) thin films that structural rearrangement/cross-linking have occurred in the chemical structure of formed thin films due to plasma polymerization process. However, the aromatic ring structure and the ethyl group of the starting monomer are

retained in PPDEA thin film. The optical band gaps (E_g) of PPDEA thin films of different thicknesses were found to be about 3.60 and 2.23 to 2.38 eV for direct and indirect transitions respectively. The change in E_g values with thickness is, due to increased structural modification in PPDEA with plasma duration. The Urbach energy, steepness parameter and extinction coefficient are also assessed for PPDEA thin films of different thicknesses from ultraviolet-visible spectroscopic data.

Akther and bhuiyan [18] investigated on dielectric properties of plasma polymerized N,N,3,5 tetramethylaniline (PPTMA) thin films in aluminium/thin film/aluminium configuration. The infrared spectroscopic analyses revealed that PPTMA thin films contained an aromatic ring structure with NC and CH side groups, presence of C=O was also evident. The differential thermal analysis and thermogravimetric analysis reveled that PPTMA thin film is thermally stable up to about 505 K. The scanning electron microscopy of PPTMA thin film showed a smooth, flawless and pinhole free surface. The capacitance and ac electrical conductance of PPTMA thin films were measured as functions of frequency ($100 < f < 105$ Hz) and temperature ($300 < T < 450$ K). The electrical conductivity is more dependent on temperature in the low frequency region than that in the high frequency region. In PPTMA thin films the conduction may be dominated by hopping of carriers between the localized states at low temperatures and thermally excited at the high temperatures. The activation energies are estimated to be about 0.05 eV in the low temperature and 0.23 eV in the high temperature. Dielectric constant decreases with the increase of frequency and that decreases with the increase of temperature but dielectric loss increases with increasing frequency with a minimum in the low frequency region. The temperature-dependence of the Cole-Cole diagram shows the existence of distribution of dielectric relaxation times in the PPTMA thin films.

Sajeev et al. [19] reported on pristine and iodine doped polyaniline thin films prepared by ac and rf plasma polymerization techniques separately for the comparison of their optical and electrical properties. The structural properties of there films were evaluated by FTIR spectroscopy and the optical band gap was estimated from UV -vis - NIR measurements, comparative studies on the structural, optical and electrical properties of ac and rf polymerization presented here .It has been found that the optical band gap of the Polyaniline thin films prepared by plasma polymerization techniques differ considerably and the band gap was further reduced by in situ doping by iodine.

The measurement on these films show higher value of electrical conductivity in the case of rf plasma polymerization thin films when compared to ac plasma polymerized thin films. Also it is found that the iodine doping enhanced conductivity of the thin films considerably .The results are compared, correlated and explained with respect to the different structure adopted under two preparation techniques.

Kumar et al [20] reported the optical and electrical properties of PPPY films deposited in the presence and absence of iodine. The conduction mechanism in the undoped PPPY film is of Schottky type.

Blaszczyk-Lezak et al. [21] reported the preparation and optical properties of plasma polymerized perylene thin films. They obtained this film as highly absorbent and fluorescent with a root mean square (rms) roughness in the range 0.3-0.4 nm. They described that the films were formed by a matrix formed by cross-linked fragments of perylene and intact molecules that confer the observed optical properties to this material. The optical and microstructural characteristics of this type of thin films make them suitable for their integration into photonic components for various applications.

Fischer et al. [22] yielded ultrathin insoluble, low-molecular-weight polymer films by the electro polymerization of *o*-methoxyaniline under self-limiting deposition conditions. Fundamental understanding of the structure/property relationships derived from the investigations can be applied to three-dimensional electrode nanoarchitectures that incorporate such electroactive coatings for enhanced charge-storage functionality.

Cherpak et al. [23] formed poly(*o*-methoxyaniline) (POMA) thin films by thermovacuum deposition in the temperature range of 350–450 °C and at a pressure of 5×10^{-5} Torr and found that the structure properties of vacuum deposited POMA are similar to those observed for the emeraldine form of polyaniline. On the basis of the dependence of conductivity on frequency they showed that hopping mechanism dominates in a polymer film and such mechanism is typical of non-ordered systems.

Liang et al. [24] demonstrated the effect of film thickness on the electrical properties of polyimide thin films prepared by spin-coat technique. With decreasing film thickness, the ε' decreased but the conduction current increased. Using IR spectroscopy, polyimide chains were found to be oriented parallel to the electrodes. The dependence of the ε' values on film thickness were explained by the orientation of polymer chains.

Zhao et al. [25] characterized the plasma polymerized 1-Cyanoisoquinoline (PPCIQ) thin films. From IR, X-ray diffraction and SEM studies it was found that a high retention of aromatic ring structure of the starting monomer was found in the films. As the films were homogeneous it was used for dielectric measurements. The dielectric measurement of PPCIQ thin film deposited at 15W gives a low ε' 2.62, which might be a potential candidate to be used as inter-metallic dielectrics in microelectronics.

Cho and Boo [26] deposited nitrogen-doped thiophene plasma polymer (N-ThioPP) thin films by radio frequency (13.56 MHz) plasma enhanced chemical vapor deposition (PECVD) method. Thiophene was used as organic precursor (carbon sorce) with hydrogen (H) gas as the precursor bubbler gas. Additionally, nitrogen gas (N_2) was used as N dopant. Furthermore, additional argon (Ar) was used as a carrier gas. The as-grown polymerized thin films were analyzed using ellipsometry, FTIR spectroscopy, Raman spectroscopy, and water contact angle (CA) measurement. The ellipsometry results showed the refractive index change of the N-ThioPP film. The FTIR spectra showed that the N-ThioPP films were completely fragmented and polymerized from thiophene. NHx species was increased by increasing the N_2 flow rate. Also, decreasing the CA shows the increasing surface energy of the N -ThioPP thin film with increasing N_2 flow rate. Additionally, decreasing the contact angle indicates the indirect cause of the increasing N amounts in the N-ThioPP thin film. N atoms bonded with thiophene molecules during the PECVD process. UV-Vis spectra of all samples show 80% of transmittance in the infrared region. However, transmittance in the visible region was dramatically changed by increasing the N amounts. Thus, the E_g of N-ThioPP was increased by increasing the N amounts.

1.3 Aim of the Present Study

Among many methods of depositing thin films of organic compounds, plasma polymerization by glow discharge can be considered as an attractive technique for the formation of new kinds of materials.This work is aimed at preparing thin films of BN by plasma polymerization and characterizing those using different physical techniques.

In the present investigation, plasma polymerized benzonitrile (PPBN) thin films would be prepared at optimized conditions by a capcitively coupled glow discharge plasma polymerization method. The chemical structure, thermal analysis, the

absorption co-efficient, optical energy gaps(E_g) and ac electrical conduction(σ_{ac}) would be investigated.

The functional groups of BN and as-deposited PPBN would be identified by FTIR spectroscopy to know the structural change due to polymerization.

Differential thermal analysis (DTA), Thermogravimetric analysis (TGA) and differential thermogravimetric analysis (DTG) of BN and PPBN were investigated to understand the thermal properties such as degradation temperature, change in weight loss of the samples, etc.

UV-Vis spectroscopy would be done to calculate the absorption coefficient and from which the direct and indirect band gaps of PPBN would be obtained.

The ac electrical measurements would be performed at different frequencies and at different temperatures on samples of different thicknesses to understand the ac conduction mechanism and dielectric relaxations in PPBN thin films. Thickness dependence of these parameters would be observed and would be analyzed. The results obtain from the ac electrical investigation would be analyzed with the existing theories to elucidate the relaxation behavior. These results in conjunction with the structural, thermal and optical analyses would help finding suitable applications of these materials in optical /electrical device.

1.4 Structure of the Thesis

This research work has been configured into five chapters in this thesis.

Chapter one presents a general introduction. A number of literatures of recent works are reviewed to understand the scientific importance of those studies need for the present investigation and the objectives of the study.

Chapter two describes the details about polymers, plasma polymers, different polymerization processes, advantages and disadvantages of plasma polymers.

The experimental techniques are briefly explained in chapter three along with the description of the plasma polymerization set up, generation of glow discharge, film thickness measurements, sample formation, etc. The monomer, substrate materials and its cleaning process are also included here. A brief description of the instrumentation of the different characterization techniques are also presented here.

The structural, thermal and optical properties are presented in chapter four. The ac electrical properties of PPBN thin films such as ac conductivity, dielectric relaxation

processes of as-deposited PPBN thin films are discussed in this chapter. The variation of ac conductivity, dielectric constant and dielectric loss tangent, with thickness and temperature are presented and finally ‘n’ values for ac conductivity, activation energy etc. are calculated to characterized the PPBN.

Finally, the conclusions of the work done and suggestions for future research on this material are included in chapter five.

2.1 Introduction

Polymeric materials have a vast potential for exciting new applications in the foreseeable future. Polymer uses are being developed in such diverse areas such as: conduction and storage of electricity, molecular based information storage and processing, molecular composites, unique separation membranes, new forms of food processing and packaging, health, housing, and transportation. Indeed, polymers will play an increasingly important role in all aspects of everyday life. The large number of current and future applications of polymeric materials has created a great interest for scientists to carry out research and development in polymer science and engineering

This chapter presents a detail of polymers their general properties and different-polymerization processes. The details of plasma, an overview of gas discharge plasma, plasma polymerization, different types of glow discharge reactors, plasma polymerization mechanism, advantages and disadvantages of plasma polymerized thin films are illustrated in this chapter. Application of plasma polymerized organic thin films is focused at the end of the chapter.

2.2 Polymers

The term „polymer" is derived from the Greek words: polys meaning many, and meros meaning parts. Polymers are a large class of materials consisting of many small molecules (called monomers) that can be linked together to form long chains, thus they are known as macromolecules. A polymer is a substance composed of molecules with large molecular mass composed of repeating structural units, or monomers, connected by covalent chemical bonds.

In some cases the repetition is linear to form linear chain, in others the chains are branched or inter connected to form three-dimensional networks. The repeat unit is usually equivalent to the monomer, or starting material from which it is formed. Polymers have anomalous properties because they were so different from the properties of low molecular weight compounds. Polymers are thought to be colloidal substances i.e. glue-like materials. From chemical point of view, the colloidal substances are in fact large molecules and their behavior could be explained in terms of the size of the individual molecules. Polymers having molecular weight roughly in the range of 1000-

20,000 are called low polymers and those having molecular weight higher than 20,000 as high polymers [27, 28].

2.2.1 Some important types of polymers

There exist many polymers or macro-molecules, which contain hundreds or thousands of atoms. Some of these are naturally occurring and some of these are manmade. Both of these cover a wide range of polymers.

Elastomers- have a loose cross-linked structure. This type of chain structure causes elastomers to possess memory. Typically, about 1 in 100 molecules are cross-linked on average. When the average number of cross-links rises to about 1 in 30 the material becomes more rigid and brittle. Natural and synthetic rubbers are both common examples of elastomers.

Addition Polymers - the monomer molecules bond to each other without the loss of any other atoms. Alkene monomers are the biggest groups of polymers in this class. Condensation Polymers - usually two different monomers combine with the loss of a small molecule, usually water. Polyesters and polyamides (nylon) are in this class of polymers.

Linear: Linear polymers are most common. They can occur whenever two reacting chains join to make a chain. If the long-chains pack regularly, side-by-side, they tend to form crystalline polymers. If the long chain molecules are irregularly tangled, the polymer is amorphous since there is no long range order. Sometimes this type of polymer is called glassy. Cross-Linking: In addition to the bonds which hold monomers together in a polymer chain, many polymers form bonds between neighboring chains. These bonds can be formed directly between the neighboring chains, or two chains may bond to a third common molecule. Though not as strong or rigid as the bonds within the chain, these cross-links have an important effect on the polymer. Polymers with a high enough degree of cross-linking have "memory." When the polymer is stretched, the cross-links prevent the individual chains from sliding past each other. The chains may straighten out, but once the stress is removed they return to their original position and the object returns to its original shape.

Homopolymers - consist of chains with identical bonding linkages to each monomer unit. This usually implies that the polymer is made from all identical monomer molecules. These may be represented as: -[A-A-A-A-A-A]-

Copolymers - consist of chains with two or more linkages usually implying two or more different types of monomer units. These may be represented as: -[A-B-A-B-A-B]-

2.2.2 Crystalline and amorphous states of polymer

Molecular shape and the way molecules are arranged in solid effects the properties of polymers. The morphology of most polymers is semi-crystalline. That is, they form mixtures of small crystals and amorphous material and melt over a range of temperature instead of at a single melting point. There are some polymers that are completely amorphous, but most are a combination with the tangled and disordered regions surrounding the crystalline areas. Such a combination is shown in the following diagram.

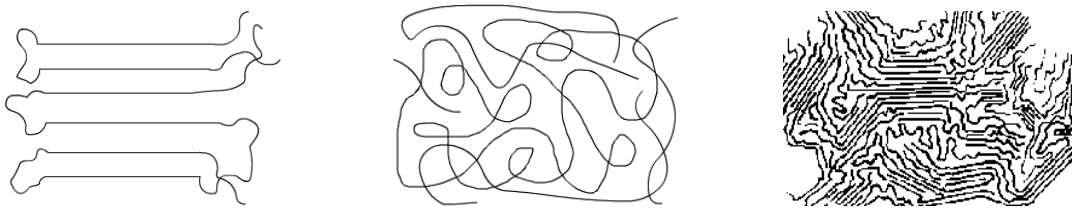

Crystalline Amorphous Semi crystalline

Fig. 2.1 Different states of Polymers

An amorphous solid is formed when the chains have little orientation throughout the bulk polymer. The glass transition temperature is the point at which the polymer hardens into an amorphous solid. This term is used because the amorphous solid has properties similar to glass.

2.3 Plasma and Plasma Polymerization

2.3.1 Plasma: The fourth state of matter

The plasma state is often referred to as the fourth state of matter. Much of the visible matter in the universe is in the plasma state. Stars, as well as visible interstellar matter, are in the plasma state. Besides the astro-plasmas, which are omnipresent in the universe, there are two main groups of laboratory plasma, i.e., the high-temperature of

fusion plasmas, and the socalled low-temperature plasma or gas discharges. In general, a subdivision can be made between plasmas which are in the thermal equilibrium and those which are not in the thermal equilibrium. Thermal equilibrium implies that the temperature of all species (electrons, ions, neutral species) is the same. High temperature is required to form these equilibrium plasmas, typically ranging from 4000 K to 20000 K. This is true for stars, as well as for fusion plasmas. On the other hand, interstellar plasma matter is typically not in thermal equilibrium [29].

Depending upon the frequency used, one decides thereby between alternating current (50 Hz), Audio (kHz) - Radio (MHz) frequency or microwave (GHz) plasmas. Plasmas get used technically, i.e. in fluorescent tubes and, above all, in recent times in the surface technique.

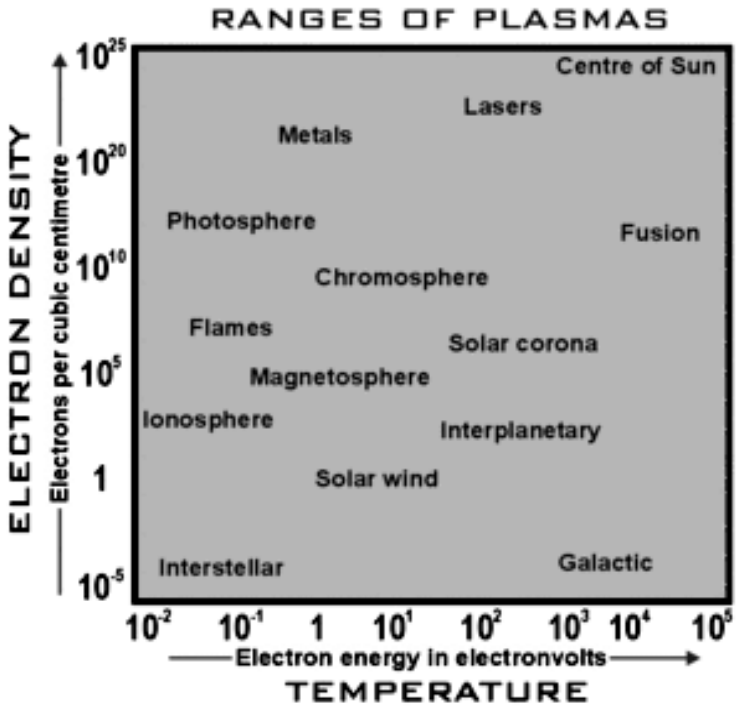

Fig. 2.2: Schematic ranges of plasma.

In recent years, the field of gas discharge plasma applications has rapidly expanded [29, 30, 31]. Because of the multi- dimensional parameter space of the plasma conditions, there exists a large variety of gas discharge plasmas employed in a large range of applications. Four types of plasma i.e., the glow discharge (GD), capacitively coupled (CC), inductively coupled plasma (ICP), and the micro wave-inductively plasma (MIP), are commonly used in plasma spectrochemistry and are

therefore familiar to most spectrochemists. However these plasmas, as well as related gas discharges, are more widely used in technological fields.

To generate the plasma, it is necessary to ionize atoms or molecules in the gas phase. When an atom or molecules gains enough energy from an external excitation source or through collisions with another molecule, ionization occurs [32]. This happens usually when the molecules are under specific conditions, like extreme heat which generates the so-called hot plasmas, or under electrical glow discharge which generates the cold plasmas [33]. The plasmas loose energy to their surroundings through collision and radiation processes; as a result, energy must be supplied continuously to the system to maintain the plasma state. The easiest way to supply energy to a system in a continuous manner is with an electrical source. Therefore, electrical glow discharges are the most common plasmas [34].

2.3.2 An overview of gas discharge plasma

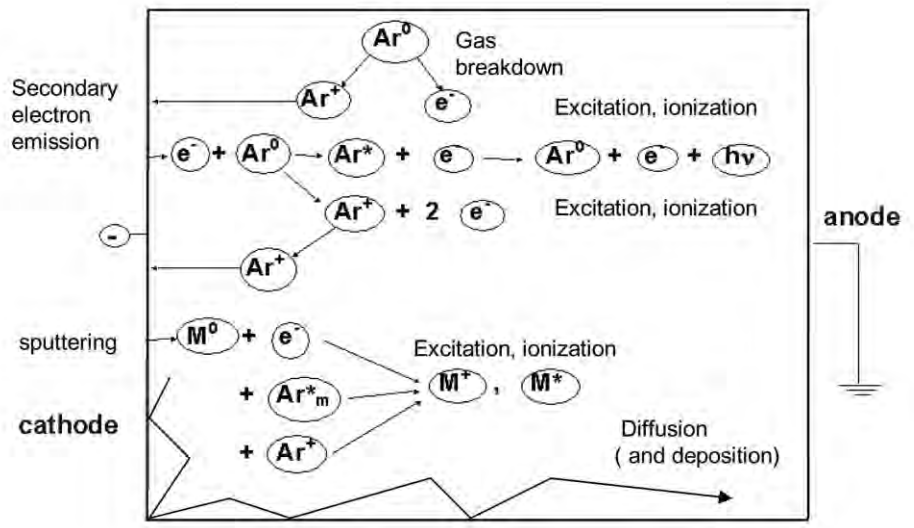

Fig. 2.3: Schematic overview of the basic processes in a glow discharge.

Plasma polymerization takes place in low temperature plasma which is provided by a glow discharge operated in an organic gas or vapor (monomer) at low pressure between two electrodes. When a sufficient high potential difference is applied between the two electrodes, the gas will break into positive ions and electrons, giving rise to a gas discharge [30, 31].

However, when a potential difference is applied the electrons are accelerated by the electric field in front of the cathode and collide with the gas atoms. The most important collisions are the inelastic collisions leading to excitation and ionization. The excitation collisions create new electrons and ions. The ions are accelerated by the electric field toward the cathode, where they release new electrons by ion-induced secondary electron emission. The electrons give rise to new ionization collisions, creating new ions and electrons. These processes of electron emission at the cathode and ionization in the plasma make the glow discharge self-sustaining plasma [35].

Another important process in the glow discharge is the phenomenon of sputtering, which occurs at sufficiently high voltage. When the ions and fast atoms from the plasma bombard the cathode, they not only release secondary electrons, but also atoms of the cathode materials, which are called sputtering. This is the basis of the use of glow discharges for analytical spectrochemistry. The ions can be detected with a mass spectrometer and the excited atoms or ions emit characteristic photons, which can be measured with optical emission spectrometry. Alternatively, the sputtered atoms can also diffuse through the plasma and they can be deposited on a substrate, this technique used in materials technology e.g. for the deposition of thin films.

2.3.3 Direct current glow discharge

When a constant potential difference is applied between the cathode and anode, a continuous current will flow through the discharge; giving rise to a direct current (dc) glow discharge. In a dc glow discharge the electrodes play an essential role for sustaining the plasma by secondary electron emission. The potential difference applied between the two electrodes is generally not equally distributed between cathode and anode, but it drops almost completely in the first millimeters in front of the cathode.

A dc glow voltage can operate over a wide range of discharge conditions. The pressure can vary from below 1 Pa to atmospheric pressure. The product of pressure and distance between the electrodes (PD) is a better parameter to characterize the discharge. For instance, at lower pressure, the distance between cathode and anode should be longer to create a discharge with properties comparable to these of high pressure with small distance. The discharge can operate in a rare gas (most often argon or helium) or in a reactive gas (N_2, O_2, H_2, CH_4, SiH_4, SiF_4, etc.), as well as in a mixture of these gases.

2.3.4 Alternating current glow discharge

In an alternating current (ac) glow discharge, the mechanism depends on the frequency of the excitation. At low frequencies, the system can be looked upon as a DC glow discharge with alternating polarity. By increasing the frequency of the applied voltage, positive ions become immobile, because they can no longer follow the periodic changes in field polarity, and only respond to time - averaged fields. At frequencies above 500 kHz, the half - cycle is so short that all electrons and ions stay within the interelectrode volume. This reduces the loss of charged particles from the system significantly, and regeneration of electrons and ions occurs within the body of the plasma through collisions of electrons with gas molecules. In radiofrequency plasma (13.56 MHz) therefore, no contact between the electrodes and the plasma is required. The plasma can be initiated and sustained by external electrodes, at a much lower voltage than is required for maintaining a direct current glow discharge [36, 37].

2.4 Deposition of Thin Films by Plasma polymerization

Thin polymer films deposited by so-called plasma polymerization, is essentially a plasma enhanced chemical vapor deposition process. It refers to the deposition of polymer films due to the excitation of an organic monomer gas and subsequent deposition and polymerization of the excited species on the surface of a substrate. Polymers formed by plasma polymerization are, in most cases, highly branched and highly cross-linking. Plasma polymerization is characterized by several features: [30-33]

- Plasma polymers are not characterized by repeating units.
- The properties of the plasma polymer are not only determined by the monomer being used, but also by the plasma parameters.
- The monomer used for plasma polymerization does not have to contain a functional group, such as a double bond.

2.4.1 Fundamental aspects of plasma polymerization

The ionization of a molecule by collision with an accelerated electron is essential process for creating plasma of a monomer (with or without carrier gas). The ionization of molecule is first elementary step of plasma polymerization and is more complex than the ionization of an atom. Conventional polymerization is highly

dependent on the structure of the monomer. However, in plasma polymerization, monomers and any organic compound without a polymerizable structure such as a double bond can polymerize. Plasma polymerization takes place through several reaction steps. In the initiation stage, free radicals and atoms are produced by collisions of electrons and ions with monomer molecules, or by dissociation of monomers adsorbed on the surface of the sample. Secondarily, the formation of the polymeric chain by the propagation of the reaction can take place both in the gas phase and on the substrate film. Finally, termination can also take place in the gas phase or at the polymer surface ending either with the final product or with a closed polymer chain.

2.4.2 Details of Plasma polymerization

In the plasma polymerization process, a monomer gas is pumped into a vacuum chamber where it is polymerized by plasma to from a thin, clear coating. The monomer starts out as a liquid. It is converted to a gas in an evaporator and is pumped into the vacuum chamber. A glow discharge initiates polymerization. The excited electrons created in the glow discharge ionize the monomer molecules. The monomer molecules break apart (fractionate) create free electrons, ions, exited molecules and radicals. The radicals absorb, condense and polymerize on the substrate.

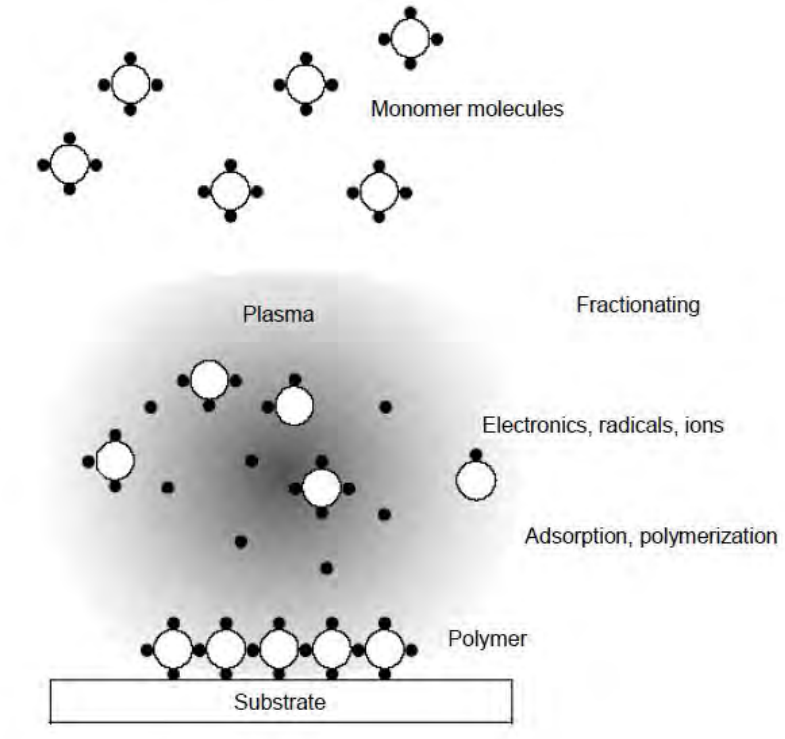

Fig.2.4: A schematic plasma polymerization configuration.

The electrons and ions crosslink, or create a chemical bond, with the already deposited molecules, creating a harder, denser coating. A schematic plasma polymerization configuration is presented in Fig. 2.4.

The materials obtained by plasma polymerization are significantly different from conventional polymers and also different from most inorganic materials. Hence plasma polymerization should be considered as a method of forming new types of materials rather than a method of preparing conventional polymers. Comparison of the structures of plasma polymers and conventional polymers is shown in the Fig. 2.5. This polymerization process covers a wide interdisciplinary area of physics, chemistry, science of interfaces and materials science and so on [38, 39]. Thus plasma polymerization is a versatile technique for the deposition of films with functional properties suitable for a wide range of modern applications. Historically, it was known that electric discharge in a glass tube forms oily or polymer-like products at the surface of the electrodes and at the wall of the glass tube. This undesirable deposit however had extremely important characteristics that are sought after in the modern technology of coating that is, i) excellent adhesion to substrate materials and ii) strong resistance to most chemicals.

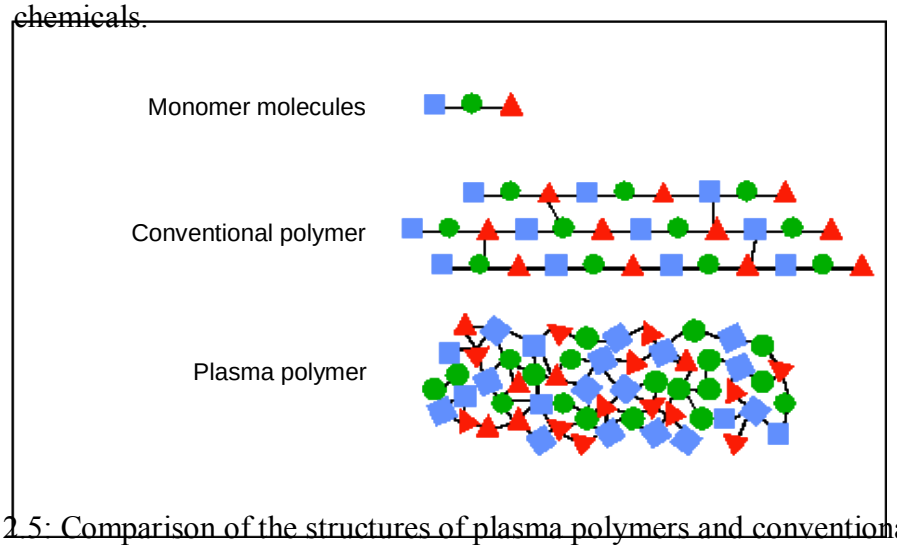

Fig. 2.5: Comparison of the structures of plasma polymers and conventional polymers.

To explain the reaction mechanism, many investigators discussed the effects of discharge conditions on polymerization rate such as polymerization time monomer pressure, discharge current, and discharge power and substrate temperature.

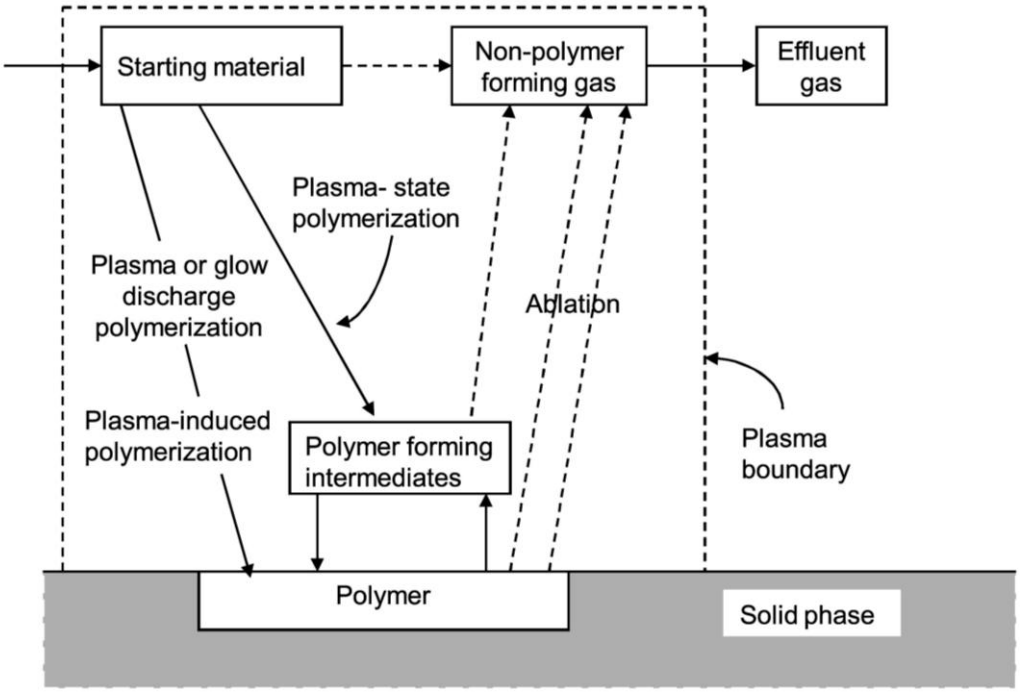

Fig. 2.6: Competitive ablation and polymerization, scheme of glow discharge polymerization.

Though, same monomer is used for polymerization, polymers formed by plasma polymerization show distinguished chemical composition and chemical and physical properties from those formed by conventional polymerization. To appreciate the uniqueness of plasma polymerization, it is useful to compare the steps necessary to obtain a good coating by a conventional coating process and by plasma polymerization. Coating a certain substrate with a conventional polymer, at least several steps are required (1) synthesis of a monomer, (2) polymerization of the monomer to form a polymer, (3) preparation of coating solution, (4) cleaning, (5) application of the coating, (6) drying of the coating and (7) curing of the coating. Polymers formed by plasma polymerization aimed at such a coating are in most cases branched and cross-linked [40-43].

Among the many types of electric discharge, glow discharge is by far the most frequently used in plasma polymerization. Some other models were proposed based on ion or electron bombardment. The role of ion bombardment is pointed to a competition between etching and deposition processes in plasma polymerization was given by Yasuda as shown in Fig.2.6.

2.5 Glow Discharge Reactors

Glow discharge reactor is the important part of plasma polymerization system. Because reactor geometry influences the extent of charge particle bombardment on the growing films which affects the potential distribution in the system.

The most widely used reactor configurations for plasma polymerization can be broadly divided in to three classes [44]:

(a) Bell jar reactors

(b) Parallel plate electrode reactors and

(c) Electrode less reactors

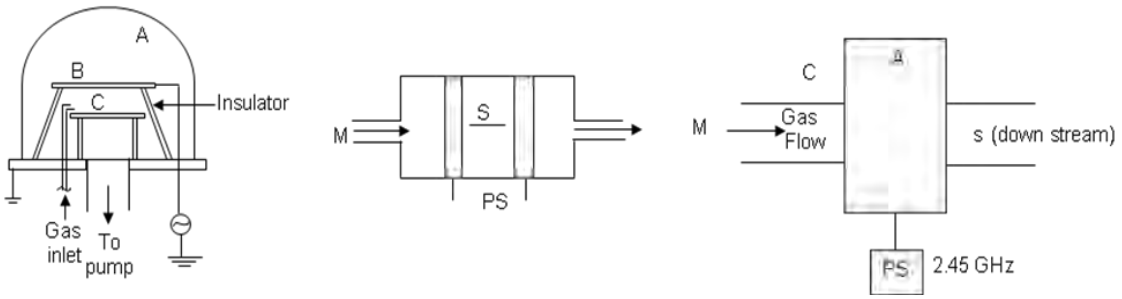

(a) (b) (c)

Fig. 2.7: Schematic structure of (a) bell jar reactor, (b) parallel plate internal electrode reactor and (c) electrode less microwave reactor.

Reactors with internal electrodes have different names, e.g. flat bed parallel plates, planar, diode etc. Their main features are power supply, coupling system, vacuum chamber, rf driver electrode, grounded electrode, and eventually one or more substrate holders. Among the internal electrode arrangements a bell-jar-type reactor with parallel plate metal electrodes is mot frequently used by using ac (1-50 kHz) and rf fields for plasma excitation.

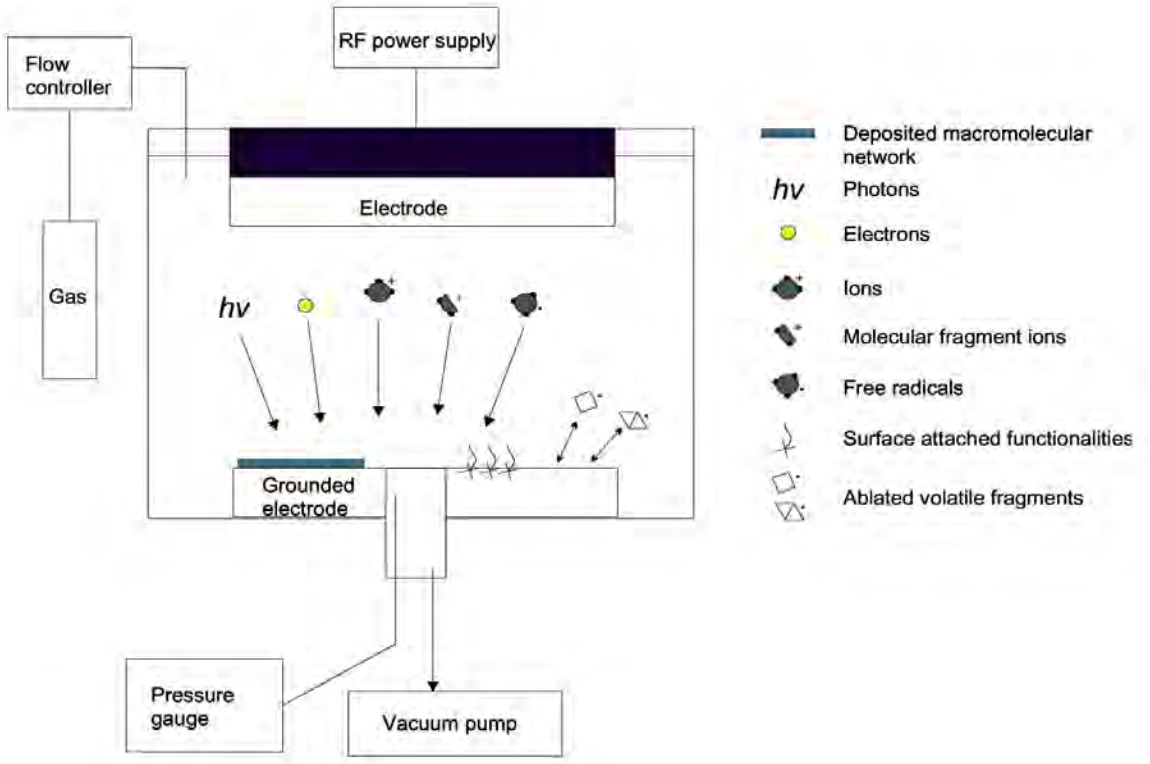

Fig. 2.8: A schematic diagram of the capacitively coupled parallel plate plasma reactor.

The vacuum chambers can be made either of glass or of conductive materials, such as metal. In the case of bell-jar reactors, no particular care is taken for the grounded electrode apart from its area. On the contrary, the design and arrangement of the cathode require special attention: a metallic shield surrounding the electrode highly improves the glow confinement inside interelectrodic space; electrode material and area greatly affect the extension of sputtering on the target.

In the current research, capacitively coupled reactor (glow discharge plasma) system was used for the formation of thin films. Figure 2.8 represents a scheme of a capacitively coupled parallel plate plasma reactor, similar to the bell jar reactor. The possible species present when the plasma is generated are also drawn. Usually plasma reactor can use internal or external electrodes. This model uses internal electrodes.

2.6 Overall Reactions and Growth Mechanism in Plasma Polymerization

The mechanism of reaction by which plasma polymerization occurs is quite complex and cannot be specifically described for the general case. Operational parameters such as monomer flow rate, pressure frequency, and power affect the deposition rate and structure of the plasma film. The electrons or atoms generated by

partial ionization of the molecules are the principle sources for transferring energy from the electric field to the gas in all glow discharges [45, 46].

In plasma polymerization, free electrons gain energy from an imposed electrical field and then transfer the energy to neutral gas molecules, which lead to the formation of many chemically reactive species. By applying greater power to the rf source, the energy per unit mass of the monomer is increased and may bring about changes in the fragmentation process. As a result, free radicals may become entrapped in the plasma-polymerized film and increase in concentration with increasing rf power. The deposition of polymer films in low-pressure plasma is a complex phenomenon involving reactions, which occur both in the plasma phase and at the surfaces bounding the plasma.

The study of plasma polymerization kinetics is commonly employed to elucidate polymerization mechanisms. With this background a comparison of the polymer formation rates of various monomers by plasma polymerization would provide an overview of the kind of reaction mechanism responsible for plasma polymerization.

The probable chain growth polymerization is represented by

$$M_n^* + M \rightarrow M^*_{n+1}$$

Where M_n^* is the reactive chain carrying species and M is the monomer molecules. But Yasuda and Lamaze [46], on the basis of their observation on plasma polymerization ruled out the chain growth polymerization. The rapid step-growth mechanism is very likely to be the reaction in plasma polymerization and this reaction is expressed as:

$$[M_m^* + M_n^* \rightarrow M_{m+n}^*] \times N$$

Where, N represents the number of repetitions of similar reactions. In this case, the reaction occurs between molecules.

In case of difunctional reactive species, *M* the overall polymerization can be represented by

$$n^*M^* \rightarrow {}^*(M_n)^*$$

If the reactive species are monofunctional (M*), such as free radical R*, the reaction is given by

$$M_m^* + M_n^* \rightarrow \quad M_{m+n}$$

This is essentially a termination process that occurs in free radical polymerization and does not contribute without additional elementary steps. Yasuda and Lamaze [46] pointed out that the reactivation of the product of an elementary reaction was bound to occur in plasma.

The overall polymerization mechanism based on the rapid step-growth principle shown in Fig. 2.9. The figure shows the overall reaction, which contains two major routes of rapid step-growth. Cycle-1 is via the repeated activation of the reaction products from monofunctional activated species, Cycle-2 is via difunctional or multifunctional activated species.

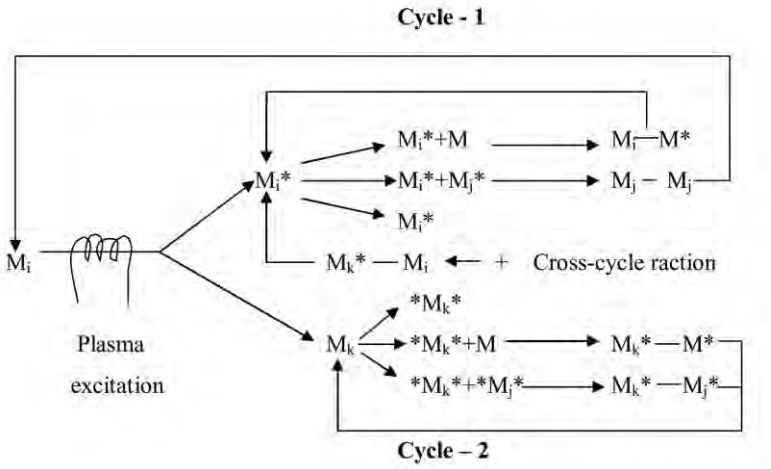

Fig. 2.9: Schematic representation of bicycle step growth mechanism of plasma polymerization.

Here, M_x refers to neutral species that can be original monomer molecule or any of the dissociation products including some atoms, such as hydrogen, chlorine, fluorine and others; M* activated species; *M* difunctional activated species and the subscripts i, j, k indicate the difference in the size of the species involved (i=j is possible, thus i=j=1 for initial monomer.)

One of the most important features of plasma polymers is that a large quantity of free radicals is often trapped in the polymer. Although, the amount varies with the type of monomer and the conditions of the plasma polymerization, it is safe to consider that plasma polymers contain a certain amount of trapped free radicals. Therefore, the free radicals play important role in plasma polymers.

In plasma polymerization, deposition rates and polymer film densities have been shown to vary with substrate temperature and discharge power. Some authors have observed that deposition rate decreases with increasing substrate temperature. Polymeric films produced by plasma polymerization have branched and cross-linked structures and are difficult to dissolve in organic solvents. Their structure is irregular and amorphous and there may be no distinction between the main chain and branches.

2.7 Advantages and Disadvantages of Plasma Polymerization

The plasma polymerization process offers several advantages over conventional polymer synthesis. Several advantages of plasma polymerized films:

- The main advantage of plasma polymerization is that it can occur at moderate temperature compared to conventional chemical reaction.
- Plasma polymerization is used to deposit films with thickness from several tens to several thousands of Angstroms.
- Plasma-polymerized films are generally chemically inert, insoluble, mechanically tough, and thermally stable.
- Consistently even, thin, clear films can be deposited.
- Time saved in the coating and curing processes and in loading, unloading and transferring parts.
- The ability to surface modify almost any substrates (glass, polymers, metals, etc.) without affecting bulk properties,
- Plasma treatment can result in changes of a variety of surface characteristics, for example, chemical, tribological, electrical, optical, biological, and mechanical. Proper applications yield dense and pinhole free coatings with excellent interfacial bonds due to the graded nature of the interface [29].
- Plasma processing can provide sterile surfaces and can be scaled up to industrial production relatively easily. On the contrary, the flexibility of non-plasma techniques for different substrate materials is smaller.
- Plasma techniques are compatible with masking techniques to enable surface patterning, a process that is commonly used in the microelectronics industry.

- Once the apparatus is set up and optimized for a specific deposition, treatment of additional substrates is rapid and simple. Through careful control of the polymerization parameters, it is possible to tailor the films with respect to specific chemical functionality, thickness, and other chemical and physical properties.

The main disadvantages of the plasma polymerization are as follows:

- Costly to retrofit equipment.
- Polymerized coatings have low abrasion resistance.
- Low deposition rates. Only very thin films can be deposited economically on high production items.
- The process doesn't discriminate against what is coated. Everything in the coating range of the polymerization process is coated, or can become part of the coating.
- The process, used in mass production, is still in its infancy. More capabilities will likely be available as improvements to the process occur.
- The chemistry produced on a surface is often not well defined, sometime a complex branched hydrocarbon polymer will be produced,
- Contamination can be a problem and care must be exercised to prevent extraneous gases, grease films, and pump oils from entering the reaction zone.

In spite of the drawbacks, plasma polymerization is far well developed process for many types of modification that simply cannot be done by any other technique.

2.8 Advantages of Plasma Polymers

The specific advantages of plasma-deposited films are summarized in here:

i) Conformal: Because of the penetrating nature of low-pressure gaseous environment in which mass transport is governed in part by both molecular (line of sight) diffusion and convective diffusion, complex geometry shapes can be treated.

ii) Pinhole-free: Under common reaction conditions, the plasma film appears to coalesce during formation into a uniform over layer free of voids. Transport property and electrical property studies suggest this continuous barrier structure.

iii) Barrier film: The pinhole-free and dense, cross-linked nature of these films suggests they have potential as barrier and protective films.

iv) Unique substrates: Plasma-deposited polymeric films can be placed upon almost any solid substrate including metals, ceramics, and semiconductors. Other surface grafting or surface modification technologies are highly dependent upon the chemical nature of the substrate.

v) Good adhesion to the substrate: The energetic nature of the gas phase species in the plasma reaction environment can induce some mixing and implantation between the film and the substrate.

vi) Unique film chemistry: The chemical structure of the polymeric over layer films produced by rf plasma deposition cannot be synthesized by conventional organic chemical methods. Complex gas phase molecular rearrangements account for these unique surface chemical compositions.

2.9 Applications of Plasma-polymerized Organic Thin Films

Plasmas are used in a large number of application fields. The most important application is probably in the microelectronics industry and in materials technology, for surface treatment, etching of surfaces (e.g., for the fabrication of integrated circuits), deposition of thin protective coatings. Applications of plasma-polymerized (PP) films are associated with biomedical uses, the textile industry, electronics, optical applications, chemical processing and surface modification [27-29]. Typical uses of plasma-polymerized films are listed below:

- In electronic industries, plasma polymerized films are used in producing integrated circuits, amorphous semiconductors, amorphous fine ceramic etching.
- These are used in fabricating insulator, thin film dielectrics, separation membrane for batteries in electrical devices.

- PP thin films are used as coating component of protective layers, hydrophobic layers, insulating layers.
- In chemical processing the films can be applied in reverse osmosis membrane, perm selective membrane, gas-separation membrane, lubrication, and insolubilization.
- In electronic industry (quartz manufacturers), and in environmental simulation (UV-radiation, ozone) pp films are used as artificial aging components.
- PP films can be used for surface modification such as in adhesive improvement, protective coating, and abrasion resistant coating, anti-crazing and scratching.
- The films are useful in anti-reflection coating, anti-dimming coating, improvement of transparency, optical fiber, optical wave-guide laser and optical window, contact lens.
- In textile industries, it has frequent use in anti-flammability, anti-electrostatic treatment, dying affinity, hydrophilic improvement, water repellence, shrink-proofing.
- In biological science the films are useful in immobilized enzymes, organelles and cells, sustained release of drugs and pesticides, sterilization and pasteurization, artificial kidney, blood vessel.

2.11 Differential Thermal Analysis

Differential thermal analysis (DTA) is a thermo-analytic technique in recording the temperature and heat flow associated with thermal transitions in a material. This enables to determine the phase transitions characteristics (e.g., melting point, glass transition temperature, crystallization etc.).In DTA the material under study and an inert reference are made to undergo identical thermal cycles, while recording any temperature difference between sample and reference. This differential temperature is then plotted against time, or against temperature (DTA curve or thermogram). Changes in the sample, either exothermic or endothermic, can be detected relative to the inert reference. Thus, a DTA curve provides data on the transformations that have occurred,

such as glass transitions, crystallization, melting and sublimation. The area under a DTA peak is the enthalpy change and is not affected by the heat capacity of the sample.

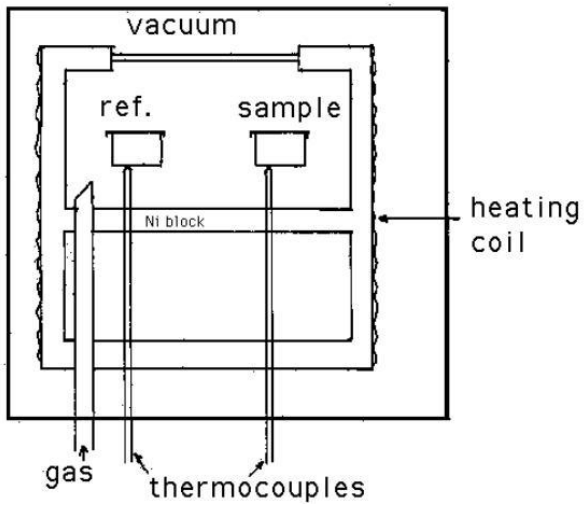

Fig. 2.10: Schematic illustration of a DTA cell.

Fig. 2.10 shows a schematic illustration of a DTA cell. It contains two holders attached with thermocouples. Sample is inserted in one holder and a reference sample is placed in the other. The difference in temperature is measured from the difference in emf between the thermocouples. These differences of temperatures appear because of the phase transitions or chemical reactions in the sample involving the evolution of heat and are known as exothermic reaction or absorption of heat known as endothermic reaction. The exothermic and endothermic reactions are generally shown in the DTA traces as positive and negative deviations respectively from a base line. So DTA offers a continuous thermal record of reactions in a sample.

2.12 Thermogravimetric analysis

Thermogravimetric analysis (TGA) is a thermal analysis technique which measures the weight change in a material as a function of temperature and time, in a controlled environment. It is suitable for use with all types of solid materials, including organic or inorganic materials .TGA is commonly employed in research and testing to determine characteristics of materials such as polymers. Sample weight changes are measured as described in Fig. 2.11.

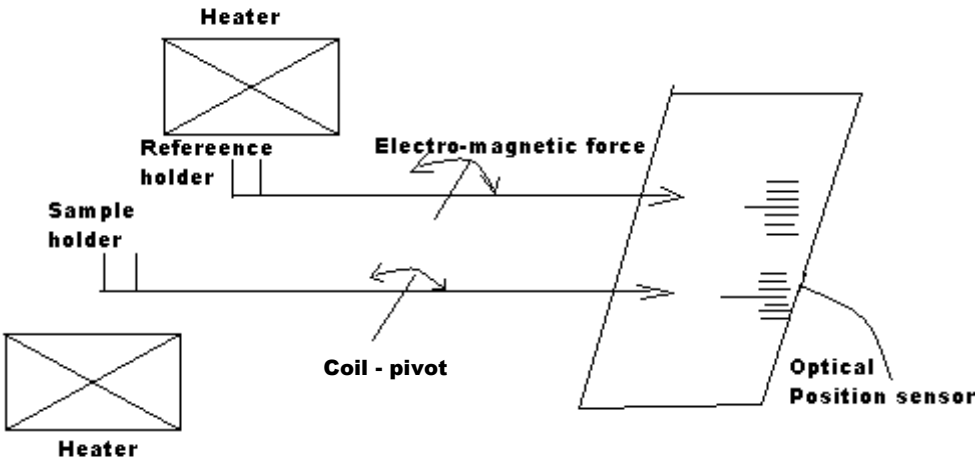

Fig. 2.11: A pictorial represention for TGA measurements.

Fig. 2.11 shows that the sample balance beam and reference balance beam are independently supported by a driving coil/pivot. When a weight change occurs at the beam end, the movement is conveyed to the opposite end of the beam via the driving coil/pivot, when optical position sensors detect changes in the position of a slit. The signal from the optical position sensor is sent to the balance circuit. The balance circuit supplies sufficient feedback current to the driving coil so that the slit returns to the balance position. The current running to the driving coils to the sample side and the current running to the driving coil on the reference side is detected and converted into weight signals.

2.13 Theory of Infrared Spectroscopy

IR Spectroscopy is an extremely effective method for determining the presence or absence of a wide variety of functional groups in a molecule. Infrared (IR) spectroscopy measures different IR frequencies by a sample positioned in the path of an IR beam and it reveals information about the vibrational states of a molecule.

The main goal of IR spectroscopic analysis is to determine the chemical functional groups in the sample. Different functional groups absorb characteristic frequencies of IR radiation and this absorption results due to the changes in vibrational and rotational status of the molecules. Actually, a molecule, when exposed to radiation produced by the thermal emission of a hot source (a source of IR energy), absorbs only

at frequencies corresponding to its molecular modes of vibration in the region of the electromagnetic spectrum between visible (red) and short waves (microwaves). These changes in vibrational motion give rise to bands in the vibrational spectrum; each spectral band is characterized by its frequency and amplitude. The absorption frequency depends on the vibrational frequency of the molecules, whereas the absorption intensity depends on how effectively the infrared photon energy can be transferred to the molecule, and this depends on the change in the dipole moment that occurs as a result of molecular vibration. As a consequence, a molecule will absorb infrared light only if the absorption causes a change in the dipole moment. Thus, all compounds except for elemental diatomic gases such as N_2, H_2 and O_2, have infrared spectra and most components present in a flue gas can be analyzed by their characteristic infrared absorption. Furthermore, using various sampling accessories, IR spectrometers can accept a wide range of sample types such as gases, liquids, and solids. Thus, IR spectroscopy is an important and popular tool for structural elucidation and compound identification.

2.13.1 Infrared frequency range and spectrum presentation

Infrared radiation spans a section of the electromagnetic spectrum having wave-numbers from roughly 3000 to 10 cm^{-1}, or wavelengths from 0.78 to 1000 μm. IR absorption positions are generally presented as either wave-numbers ($\bar{\nu}$) or wavelengths (λ). Thus, wave-numbers are directly proportional to frequency, as well as the energy of the IR absorption. In the contrast, wavelengths are inversely proportional to frequencies and their associated energy. Wave-numbers and wavelengths can be inter-converted using the following equation:

$$\bar{\nu}(cm^{-1}) = \frac{1}{\lambda(\mu m)} \times 10^4 \quad \text{.....} \quad (2.1)$$

$$A = \log_{10}(1/T) = \log_{10}(I_0 / I\ ) \quad \text{.....} \quad (2.2)$$

Table 2.1: Three smaller areas in IR region.

	Near IR	Mid IR	Far IR
Wavenumber	13000 – 4000 cm^{-1}	4000 – 200 cm^{-1}	200 – 10 cm^{-1}
Wavelength	0.78 – 2.5 μm	2.5 – 50 μm	50 – 1000 μm

The IR region is commonly divided into three smaller areas: near IR, mid IR, and far IR.The region of most interest for chemical analysis is the mid-infrared region (4,000 cm^{-1} to 400 cm^{-1}) which corresponds to changes in vibrational energies within molecules. The far infrared region (400 cm^{-1} to 10 cm^{-1}) is useful for molecules containing heavy atoms such as inorganic compounds but requires rather specialized experimental techniques. The far- and near IR are not frequently employed because only skeletal and secondary vibrations (overtones) occur in these regions producing spectra that are difficult to interpret.

2.13.2 Infrared absorption

At temperatures above absolute zero, all the atoms in molecules are in continuous vibration with respect to each other. When the frequency of a specific vibration is equal to the frequency of the IR radiation directed on the molecule, the molecule absorbs the radiation.

For a molecule to absorb IR, the vibrations or rotations within a molecule must cause a net change in the dipole moment of the molecule. The alternating electrical field of the electromagnetic radiation interacts with fluctuations in the dipole moment of the molecule. If the frequency of the radiation matches the vibrational frequency of the molecule then radiation will be absorbed, causing a change in the amplitude of molecular vibration. The energy of a molecule consists of translational, rotational, vibrational and electronic energy

$$\mathbf{E = E_{electronic} + E_{vibrational} + E_{rotational} + E_{translational}}$$

Translation energy of a molecule is associated with the movement of the molecule as a whole, for example in a gas. Rotational energy is related to the rotation of the molecule, whereas vibrational energy is associated with the vibration of atoms

within the molecule. Finally, electronic energy is related to the energy of the molecule's electrons.

Like radiant energy, the energy of a molecule is quantized too and a molecule can exist only in certain discrete energy levels. Within an electronic energy level a molecule has many possible vibrational energy levels. The vibrational energy of a molecule is not determined by the orbit of an electron but by the shape of the molecule, the masses of the atoms and, eventually by the associated vibronic coupling. For example, simple diatomic molecules have only one bond allowing only stretching vibrations. More complex molecules may have many bonds, and vibrations can be conjugated. The atoms in a CH_2 group, commonly found in organic compounds, can vibrate in six different ways: symmetrical and antisymmetrical stretching, scissoring, rocking, wagging and twisting.

The major types of molecular vibrations are stretching and bending. The various types of vibrations are illustrated in Fig. 2.12 and Fig. 2.13. Infrared radiation is absorbed and the associated energy is converted into these types of motions. The absorption involves discrete, quantized energy levels. However, the individual vibrational motion is usually accompanied by other rotational motions. These combinations lead to the absorption bands, not the discrete lines, commonly observed in the mid IR region.

Stretching: Change in inter-atomic distance along bond axis. There are two types of Stretching vibrations: Symmetric and Asymmetric.

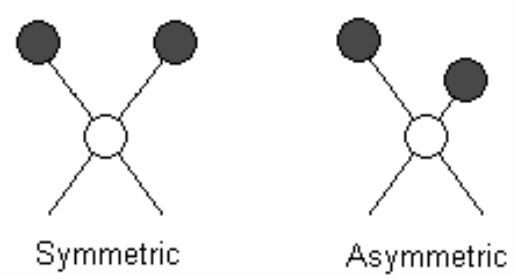

Fig. 2.12: Stretching vibrations

Bending: Change in angle between two bonds. There are four types of bend: Rocking, Scissoring , Wagging , Twisting.

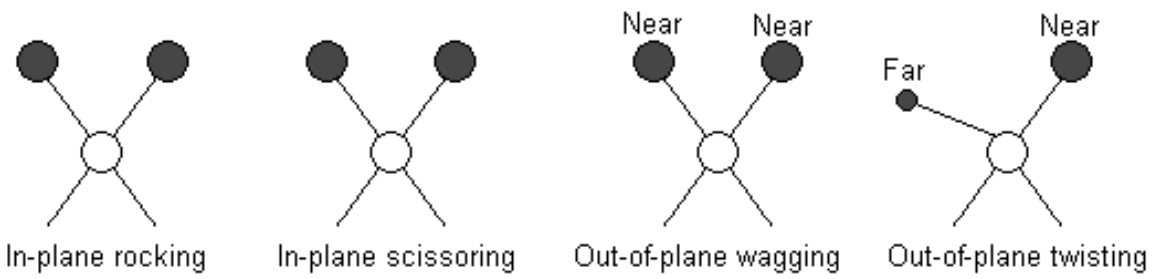

Fig. 2.13: Bending vibrations

In general, a polyatomic molecule with n atoms has 3n – 6 distinct vibrations. Each of these vibrations has an associated set of quantum states and in IR spectroscopy the IR radiation induces a jump from the ground (lowest) to the first excited quantum state. Although approximate, each vibration in a molecule can be associated with motion in a particular group.

2.14 Theory of Ultraviolet-Visible Spectroscopy

The wavelength of light that a compound will absorb is the characteristic of its chemical structure. Specific regions of the electromagnetic spectrum are absorbed by exciting specific types of molecular and atomic motion to higher energy levels. Absorption of visible and ultraviolet (UV) radiation is associated with excitation of electrons, in both atoms and molecules, to higher energy states. Most molecules required very high energy radiation. Light in the UV-visible (UV-Vis) region is adequate for molecules containing conjugated electron systems and as the degree of conjugation increases, the spectrum shifts to lower energy.

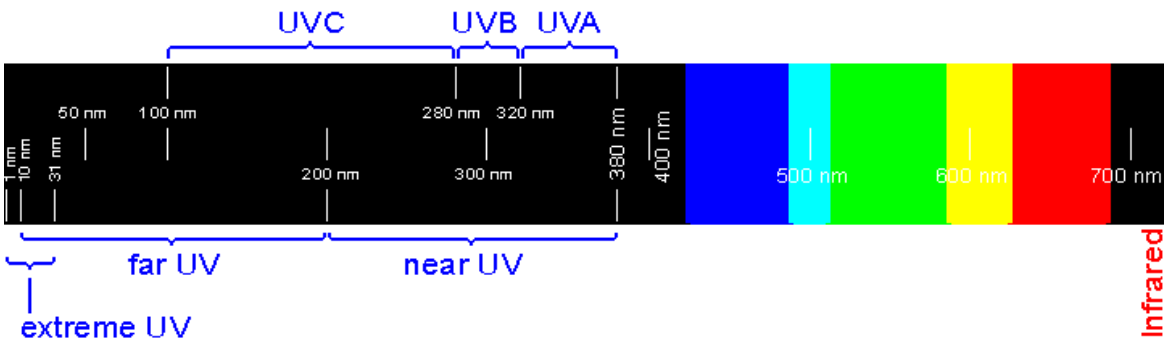

Fig 2.14: Light Spectrum

When a molecule absorbs UV-vis radiation, the absorbed energy excites an electron into an empty, higher energy orbital. This Absorption of UV-Vis radiation in organic molecules is restricted to certain functional groups (chromophores) that contain valence electrons of low excitation energy. The spectrua of a molecule containing these chromophores is complex. This is because the superposition of rotational and vibrational transitions on the electronic transitions gives a combination of overlapping lines. This appears as a continuous absorption band.

Possible electronic transitions of π, σ, and n electrons are:

$\sigma \rightarrow \sigma^*$ transitions: An electron in a bonding σ orbital is excited to the corresponding antibonding orbital. The energy required is large. For example, methane (which has only C-H bonds, and can only undergo $\sigma \rightarrow \sigma^*$ transitions) shows an absorbance maximum at 125 nm. Absorption maxima due to $\sigma \rightarrow \sigma^*$ transitions are not seen in typical UV-Vis. spectra (200 - 700 nm).

$n \rightarrow \sigma^*$ Transitions: Saturated compounds containing atoms with lone pairs (non-bonding electrons) are capable of $n \rightarrow \sigma^*$ transitions. These transitions usually need less energy than $\sigma \rightarrow \sigma^*$ transitions. They can be initiated by light whose wavelength is in the range 150 - 250 nm. The number of organic functional groups with $n \rightarrow \sigma^*$ peaks in the UV region is small.

$n \rightarrow \pi^*$ and $\pi \rightarrow \pi^*$ Transitions: Most absorption spectroscopy of organic compounds is based on transitions of n or π electrons to the π^* excited state. This is because the absorption peaks for these transitions fall in an experimentally convenient region of the spectrum (200 - 700 nm). These transitions need an unsaturated group in the molecule to provide the π electrons.

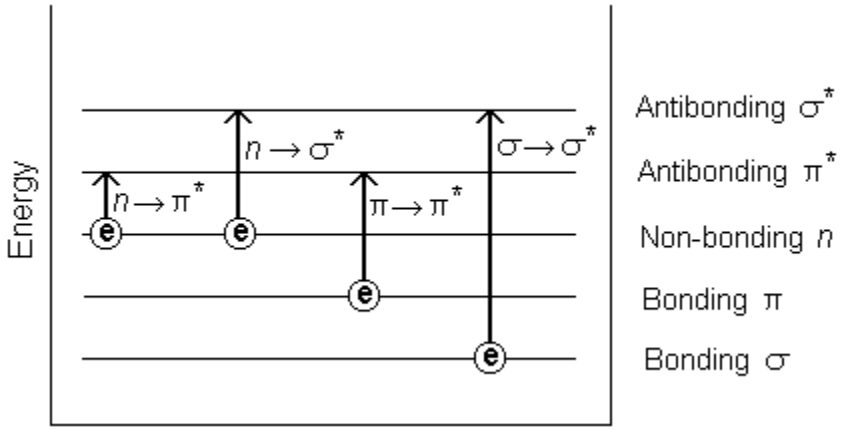

Fig. 2.15: Summery of electronic energy levels

The solvent in which the absorbing species is dissolved also has an effect on the spectrum of the species. Peaks resulting from $n \rightarrow \pi^*$ transitions are shifted to shorter wavelengths (blue shift) with increasing solvent polarity. Often (but not always), the reverse (i.e. red shift) is seen for $\pi \rightarrow \pi^*$ transitions. This is caused by attractive polarisation forces between the solvent and the absorber, which lower the energy levels of both the excited and unexcited states.

2.14.1 Direct and Indirect optical transitions

Materials are capable of emitting visible luminescence when subjected to some form of excitation such as UV light. The E-k diagrams for a direct band gap material and an indirect gap material is schematically illustrated in Fig. 2.16, where E and k are respectively the kinetic energy and wave vector of the electron or hole ($E = k^2\hbar^2 / 2m$, where $\hbar = h/2\pi$ and m is the electron or hole effective mass) .The shaded states at the bottom of the conduction band and the empty states at the top of the valence band respectively represent the electrons and holes created by the absorption of an UV or visible photon with an energy $\hbar\omega_{exc}$ exceeding the band gap E_g of the material, an electron-hole pair is created and the electron (hole) is excited to states high up in the conduction (valence) band.

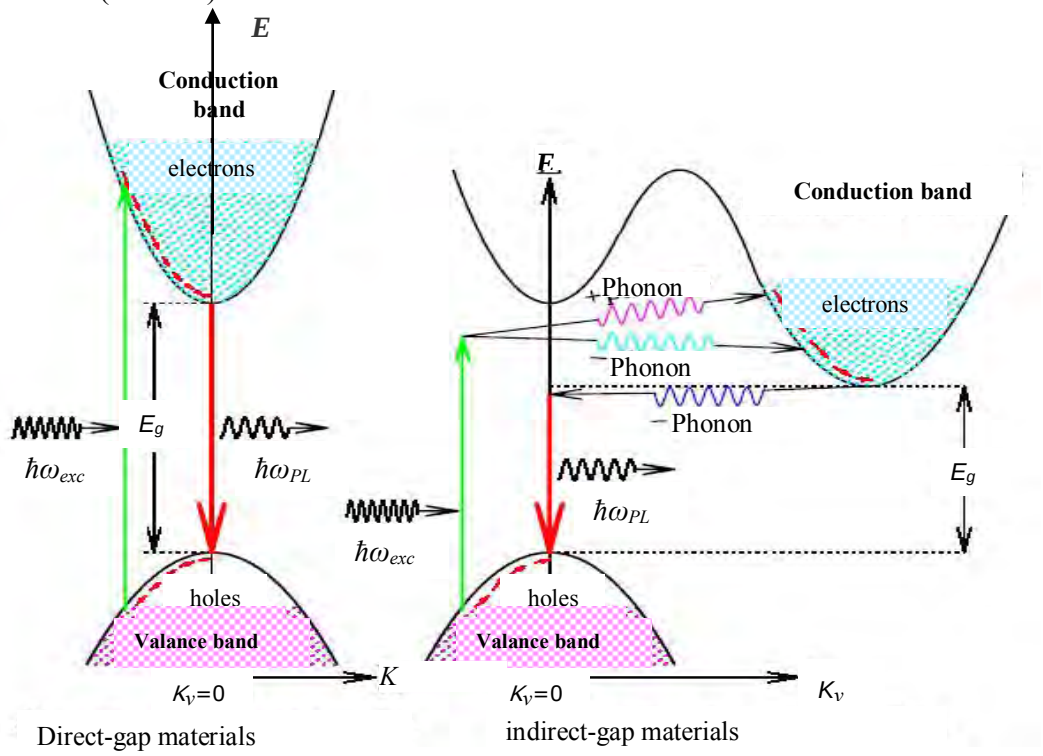

Fig. 2.16: Schematic band diagrams for the photoluminescence processes in a direct gap material (left) and an indirect gap material (right).

In a direct gap material (left), the conduction band minimum and the valence band maximum occur at the same k values which implies that the electron wave vector should not change significantly during a photon absorption process i.e., $\hbar\vec{\mathbf{k}}_{\mathbf{i}} + \hbar\vec{\mathbf{k}}_{\mathbf{phot}} \approx \hbar\vec{\mathbf{k}}_{\mathbf{i}} = \hbar\vec{\mathbf{k}}_{\mathbf{f}}$, since the wave vector of the absorbed photon $\vec{k}_{phot}$ is negligible compared to the electron wave vector. This is represented by photon absorption and emission processes by vertical arrows on E-k diagrams.

In contrast, for an indirect band gap material, of which the conduction band minimum and the valence band maximum have different k values, conservation of momentum implies that the photon absorption process must be assisted by either absorbing (indicated by a "+" sign) or emitting (indicated by a "-" sign) a phonon (a quantum of lattice vibration), because the electron wave vector must change significantly in jumping from the valence band in state (E_i, $\vec{\mathbf{k}}_{\mathbf{i}}$) to a state ($E_f$, $\vec{\mathbf{k}}_{\mathbf{f}}$) in the conduction band, and the absorption of a photon alone can not provide the required momentum change since $\left|\vec{\mathbf{k}}_{\mathbf{phot}}\right| << \left|\vec{\mathbf{k}}_{\mathbf{i}} - \vec{\mathbf{k}}_{\mathbf{f}}\right|$.

2.14.2 The Beer-Lambert law

The absorption spectrum can be analyzed by Beer-Lambert law [53], which governs the absorption of light by the molecules. It states that, “When a beam of monochromatic radiation passes through a homogeneous absorbing medium the rate of decrease in intensity of electromagnetic radiation in UV-Vis region with thickness of the absorbing medium is proportional to the intensity coincident radiation”. If I_o is the intensity of the incident radiation, I is the intensity of the transmitted radiation

$$I = I_0 e^{-\alpha d} \quad \text{.....(2.3)}$$

$$\log_e\left(\frac{I_0}{I}\right) = \alpha d \quad \text{.....(2.4)}$$

Where d is the path length of the absorbing species and α is the absorption coefficient.

Thus the absorption co-efficient, α can be calculated from the absorption data as [53-54,]

$$\alpha = \frac{2.303A}{d} \quad \text{..... (2.5)}$$

Where $A = \log_{10}\left(\frac{I_0}{I}\right)$ is the Absorbance.

The relation of extinction co-efficient k with α is

$$\alpha = \frac{4\pi k}{\lambda} \quad \text{.....(2.6)}$$

Where λ is the wavelength.

To estimate the nature of absorption a random phase model is used where the momentum selection rule is completely relaxed. The integrated density of states N(E) has been used and defined by

$$N(E) = \int_{-\infty}^{+\infty} g(E)dE \quad \text{..... (2.7)}$$

The density of states per unit energy interval may be represented by $g(E) = \frac{1}{V}\sum \delta(E - E_n)$, where V is the volume, E is energy at which g(E) is to be evaluated and E_n is the energy of the nth state.

If $g_v \propto E^p$ and $g_c(E) \propto (E\text{-}E_{opt})^q$, where energies are measured from the valance band mobility edge in the conduction band (mobility gap), and substituting these values into an expression for the random phase approximation, the relationship obtained $\nu^2 I_2(\nu) \propto (h\nu\text{-}E_o)^{p+q+1}$, where $I_2(\nu)$ is the imaginary part of the complex permittivity. If the density of states of both band edges is parabolic, then the photon energy dependence of the absorption becomes $\alpha\nu \propto \nu^2 I_2(\nu) \propto (h\nu\text{-}E_{opt})^2$. So for higher photon energies the simplified general equation is

$$\alpha h\nu = B(h\nu - E_{opt})^n \quad \text{.....(2.8)}$$

where hν is the energy of absorbed light(h is the planc constant,V is the frequency of individual radiation) , n is the parameter connected with distribution of the density of stales and B is the proportionality factor. The index n equals 1/2 and 2 for allowed direct transition and indirect transition energy gaps respectively [54].

Thus, from the straight-line plots of $(\alpha h\nu)^2$ versus hν and $(\alpha h\nu)^{1/2}$ versus hν the direct and indirect energy gaps of insulators and/or dielectrics can be determined.

2.14.3 UV-Vis spectrophotometer

In this work a dual-beam UV-Vis spectrophotometer is used and a schematic diagram of the dual-beam UV-VIS spectrophotometer is given in Fig. 2.17. The functioning of this instrument is relatively straightforward. A beam of light from a visible and/or UV light source is separated into its component wavelengths by a prism or diffraction grating. Each monochromatic (single wavelength) beam in turn is split into two equal intensity beams by a half-mirrored device. One beam, the sample beam (colored magenta), passes through a small transparent container (cuvette) containing a solution of the compound being studied in a transparent solvent. The other beam, the reference (colored blue), passes through an identical cuvette containing only the solvent. The intensities of these light beams are then measured by electronic detectors and compared. The intensity of the reference beam, which should have suffered little or no light absorption, is defined as $\mathbf{I_0}$. The intensity of the sample beam is defined as **I**. Over a short period of time, the spectrometer automatically scans all the component wavelengths in the manner described. The ultraviolet (UV) region scanned is normally from 200 to 400 nm, and the visible portion is from 400 to 800 nm.

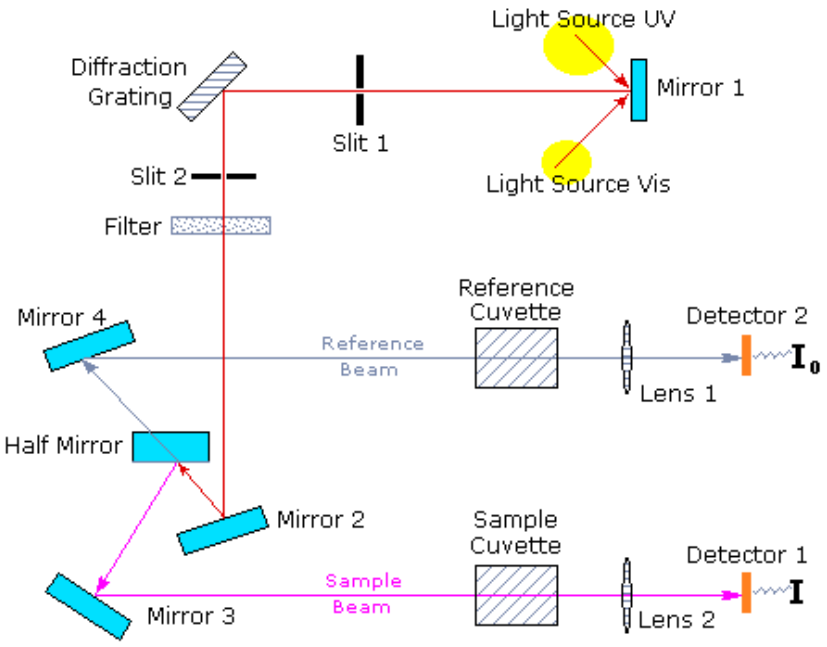

Fig. 2.17: Schematic diagram of a dual-beam UV-VIS spectrophotometer

If the sample compound does not absorb light of a given wavelength, $I = I_0$. However, if the sample compound absorbs light then I is less than I_0, and this difference may be plotted on a graph absorption versus wavelength. Absorption may be presented as

transmittance ($T = I/I_0$) or absorbance ($A = \log I_0/I$). If no absorption has occurred, T = 1.0 and A= 0. Most spectrometers display absorbance on the vertical axis, and the commonly observed range is from 0 (100% transmittance) to 2 (1% transmittance). The wavelength of maximum absorbance is a characteristic value, designated as λ_{max}.

2.15 The Theory of Dielectrics

The capacitance of a parallel plate capacitor having a dielectric medium is expressed as

$$C = \frac{\varepsilon_o \varepsilon' A}{d} \quad \text{.....(2.9)}$$

Where ε_0 is the permittivity of free space, ε' is the dielectric constant of the medium, A is the surface area of each of the plates/electrodes and d is the thickness of the dielectric.

A real capacitor can be represented with a capacitor and a resistor. The parameters such as angular frequency (ω) of The applied field, the parallel resistance $R_{P,}$ parallel capacitance C_p and the series resistance R_S and series capacitance C_s are related to the dielectric constant ε', dielectric dissipation factor ε'' and loss tangent as:

$$\varepsilon' = \frac{C_p}{C_0} \quad \text{.....(2.10)}$$

$$\varepsilon'' = \frac{1}{R_p C_0 \omega} \quad \text{.....(2.11)}$$

and

$$\tan\delta = \frac{\varepsilon''}{\varepsilon'} = \frac{1}{R_p C_p \omega} = G_p / 2\pi f C_p \quad \text{.....(2.12)}$$

The ac conductivity, σ_{ac}, was calculated using eqn.

$$\sigma_{ac} = G_p d/A \quad \text{.....(2.13)}$$

The dependence of ac conductivity, σ_{ac}, on frequency may be described by the power law [55]:

$$\sigma_{ac}(\omega) = A\omega^n \quad \text{.....(2.14)}$$

where A is a proportionality constant and ω (=2πf, f is the linear frequency) is the angular frequency and n is The exponent, which generally takes the value less than

unity for Debye type mechanism and is used to understand the conduction/relaxation mechanism in amorphous materials.

The dielectric behavior of a material is usually described by Debye dispersion equation [56, 57]:

$$\varepsilon^*(\omega,T) = \varepsilon' - i\varepsilon'' \quad \text{.....(2.15)}$$

where ε^* is the complex dielectric permittivity, ε' (energy dissipated per cycle) is the real part of complex dielectric permittivity and ε'' (energy stored per cycle) is the imaginary part of the complex dielectric permittivity.

$$\varepsilon' = \varepsilon_\infty + \frac{\varepsilon_s - \varepsilon_\infty}{1+\omega^2\tau^2} \quad \text{.....(2.16)}$$

$$\varepsilon'' = \frac{(\varepsilon_s - \varepsilon_\infty)\omega\tau}{1+\omega^2\tau^2} \quad \text{.....(2.17)}$$

where ε_s is the static dielectric constant, ε_∞ is the high frequency dielectric constant and the quantity τ is a characteristic time constant, usually called the dielectric relaxation time, it refers to a gradual change in the polarization following an abrupt change in applied field.

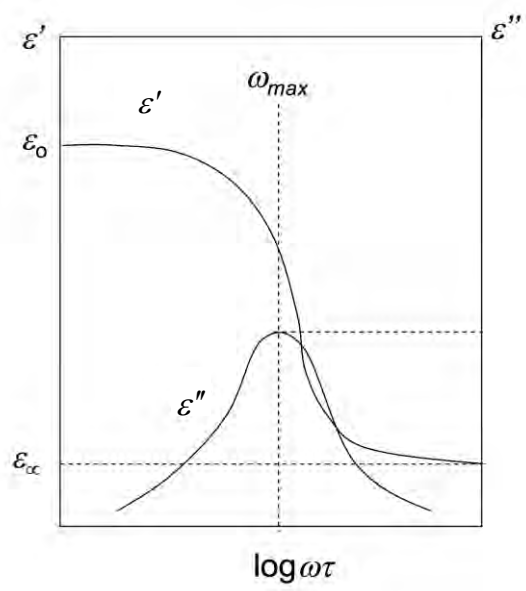

Fig. 2.18: Debye dielectric dispersion curves.

The dielectric loss tangent is expressed by

$$\tan\delta = \frac{\varepsilon''}{\varepsilon'} \quad \text{.....(2.18)}$$

The graphs of ε' and ε'' against frequency of the applied field (logarithmic scale) through the dispersion regions show that the maximum loss value occurs when $\omega\tau$ = 1, corresponding to a critical frequency $\omega_{max} = 1/\tau$, and location of this peak provides the easiest way of obtaining the relaxation time from the experimental results.

3.1 Introduction

Plasma polymerization of PPBN including the details of monomer and substrate, capacitively coupled glow discharge plasma polymerization set up for polymer formation, thickness measurement method, contact electrode deposition technique for electrical measurement and experimental of different properties measurement of PPBN thin films are discussed in this chapter.

3.2 The Monomer

Benzonitrile is the chemical compound with the formula C6H5-CN, abbreviated PhCN. This aromatic organic compound is colourless, with a sweet almond odour. It is prepared by the dehydration of Benz amide, or by the reaction of sodium cyanide with bromobenzene.

Benzonitrile is a liquid with freezing point -13 °C.Benzonitrile possesses one Benzo group and one Benzine group. The monomer Benzonitrile is manufactured by BDH Chemicals Ltd., TCL, and Japan and is collected from local market. The chemical structure of the monomer is shown in Fig. 3.1 and its typical properties are stated below:

Table 3.1 Different Parameters of Benzonitrile

Commercial Name	CN-Benzene
IUPAC name	2-cyanobenzene
Form	Clear liquid
Color	Colorless
Molecular formula	C_6H_5CN
Molecular weight	103.04 g/mol
Density	1.0 g/ml
Freezing point	-13 °C
Boiling point	188–91 °C
Vapor pressure	25°C: 102
Flash point	75 °C
Auto-ignition temperature	550 °C
Refractive index (nD)	1.528

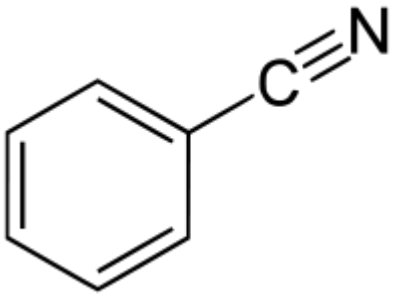

Fig. 3.1: Chemical Structure of Benzonitrile (BN)

3.3 Substrate Materials and its Cleaning Process

The substrates used were pre-cleaned glass slides (25.4 mm × 76.2 mm × 1.2 mm) of Sail Brand Japan, purchased from TCL. The samples were prepared by depositing the PPBN thin film and contact electrodes onto substrates.

To get homogeneous, smooth and flawless thin polymer film, which is a common property of plasma polymers, it is essential to make the substrate as clean as possible. The substrates were chemically cleaned by acetone and thoroughly rinsed with distilled water then dried in hot air.

3.4 Capacitively Coupled Plasma Polymerization Set-up

Glow discharge plasma and the plasma polymerization setup has been used enormously in recent years to form various kinds of plasma polymers. Different configuration of polymerization set up varies the properties of plasma polymers i.e., the geometry of the reaction chamber, position of the electrodes, nature of input power etc.

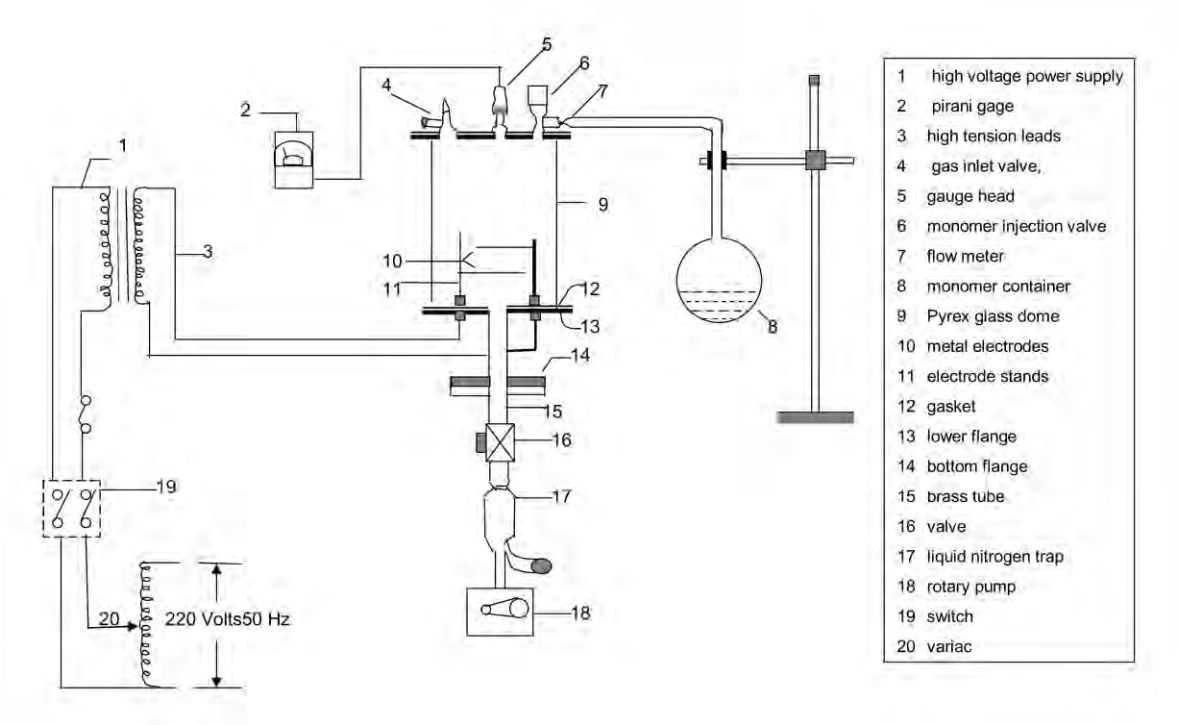

Fig. 3.2: A schematic diagram of the plasma polymerization set-up.

Fig. 3.3: The plasma polymerization set-up

The glow discharge plasma polymerization setup used to deposit the PPBN thin films consists of different components are shown in Fig.3.2 and Fig. 3.3.

Plasma reaction chamber

The glow discharge reactor is made up of a cylindrical Pyrex glass bell-jar having 0.15 m in inner diameter and 0.18 m in length. The top and bottom edges of the glass bell-jar are covered with two rubber L -shaped (height and base 0.015 m, thickness 0.001 m) gaskets. The cylindrical glass bell jar was placed on the lower flange. The lower flange is well fitted with the diffusion pump by an 'I' joint. The upper flange is placed on the top edge of the bell-jar. The flange is made up of brass having 0.01 m in thickness and 0.25 m in diameter. On the upper flange a laybold pressure gauge head, Edwards high vacuum gas inlet valve and a monomer injection valve are fitted. In the lower flange two highly insulated high voltage feed-through are attached using screwed copper connectors of 0.01m high and 0.004 m in diameter via Teflon™ insulation.

Electrode system

A capacitively coupled electrode system is used in the system. Two circular stainless steel plates of diameter 0.09 m and thickness of 0.001m are connected to the high voltage copper connectors. The inter-electrode separation can be changed by moving the electrodes through the electrode stands. After adjusting the distance between the electrodes they are fixed with the stands by means of screws. The substrates were kept on the lower electrode for plasma deposition.

Pumping unit

For creating laboratory plasma, first step is pumping out the air/gas from the plasma chamber. In this system a rotary pump of vacuubrand (Vacumbrand GMBH & Co: Germany) is used.

Vacuum pressure gauge

A vacuum pressure gauge head (Laybold AG, Germany) and a gauge meter (ThermotronTM 120) are used to measure inside pressure of the plasma deposition chamber.

Input power for plasma generation

The input power supply for plasma excitation comprises of a step-up high-tension transformer and a variac. The voltage ratio at the output of the high-tension transformer is about 16 times that of the output of the variac. The maximum output of the variac is 220V and that of the transformer is about 3.5 KV with a maximum current of 100 mA. The deposition rate increases with power at first and then becomes independent of power at high power values at constant pressure and flow rate.

Monomer injecting system

The monomer injecting system consists of a conical flask of 25 ml capacity and a Pyrex glass tube with capillarity at the end portion. The capillary portion is well fitted with metallic tube of the nozzle of the high vacuum needle valve. The conical flask with its components is fixed by stand-clamp arrangement.

Supporting frame

A metal frame of dimension 1.15 m × 0.76 m × 0.09 m is fabricated with iron angle rods, which can hold the components described above. The upper and lower bases of the frame are made with polished wooden sheets. The wooden parts of the frame are varnished and the metallic parts are painted to keep it rust free. The pumping unit is placed on the lowed base of the frame. On the upper base a suitable hole is made in the wooden sheet so that the bottom flange can be fitted with nut and bolts.

Flowmeter

The system pressure of a gas flow is determined by the feed in rate of a gas and the pumping out rate of a vacuum system. The monomer flow rate is determined by a flowmeter. In the plasma polymerization set up a flowmeter (Glass Precision Engineering LTD, Meterate, England) is attached between the needle valve and the monomer bottle.

Liquid nitrogen trap

Cold trap, particularly a liquid N_2 trap, acts as a trap pump for different type gas. The liquid N_2 trap system is placed in the fore line of the reactor chamber before the pumping unit in the plasma deposition system. It consists of a cylindrical shape chamber having 6.4 cm diameter and 11.5 cm in length using brass material.

3. 5 Deposition of Plasma Polymerized Thin Film

The important feature of glow discharge plasma considered for the purpose of plasma polymerization is the non-equilibrium state of the overall system. In the plasmas, most of the negative charges are electrons and most of the positive charges are ions. Due to large mass difference between electrons and ions, the electrons are very mobile as compared to the nearly stationary positive ions and carry most of the current. Energetic electrons as well as ions, free radicals, and vacuum ultraviolet light can possess energies well in excess of the energy sufficient to break the bonds of typical organic monomer molecules which range from approximately 3 to 10 eV. Some typical energy of plasma species available in glow discharge as well as bond energies encountered at pressure of approximately 0 .01 mbar.

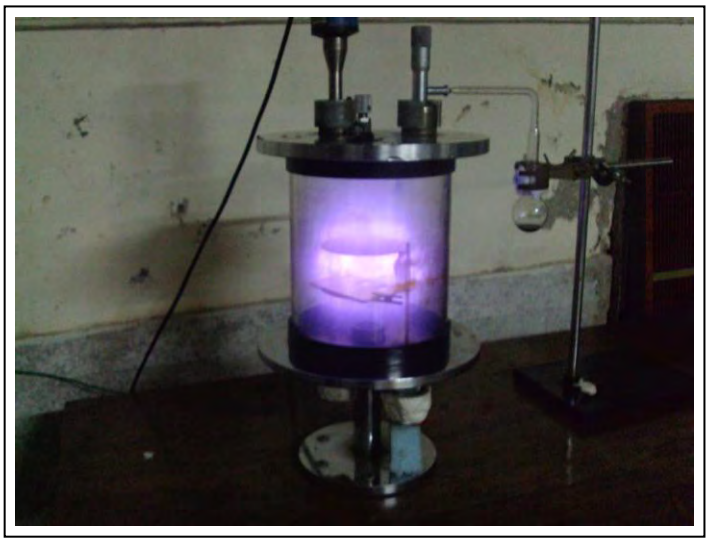

Fig. 3.4: Glow discharge plasma during deposition

The chamber of the glow discharge reactor is evacuated to about 0.01 mbar. A high-tension transformer along with a variac is connected to the feed-through attached to the lower flange. While increasing the applied voltage, the plasma is produced across the electrodes at around 0.15-mbar-chamber pressure. After finding the desired plasma glow in the reactor the monomer vapor is injected downstream to the primary air glow plasma for some time. Incorporation of monomer vapor changed the usual color of plasma into a light bluish color as shown in Fig. 3.4. The deposition time was varied

from 45-90 minutes to get the PPBN thin films of different thicknesses. The optimized conditions of thin film formation for the present study are:

Table 3.2: The optimum plasma polymerization condition for PPBN

Separation between two parallel plateelectrodes	4 cm
Position of the substrate	Lower electrode
Deposition power	40 W
Pressure in the reactor before monomer feeding	1.33 Pa
Maximum deposition time	1 hr 15 min

3.6 Contact Electrodes for Electrical Measurements

Electrode material

Aluminium (Al) (purity of 4N British Chemical Standard) was used for electrode deposition. Al has been reported to have good adhesion with glass slides [52]. Al film has advantage of easy self-healing burn out of flaws in sandwich structure [53].

Fig. 3.5: The Edward vacuum coating unit E306A.

Electrode deposition

Electrodes were deposited using an Edward coating unit E-306A (Edward, UK). The system was evacuated by an oil diffusion pump backed by an oil rotary pump. The chamber could be evacuated to a pressure less than 10^{-5} Torr.

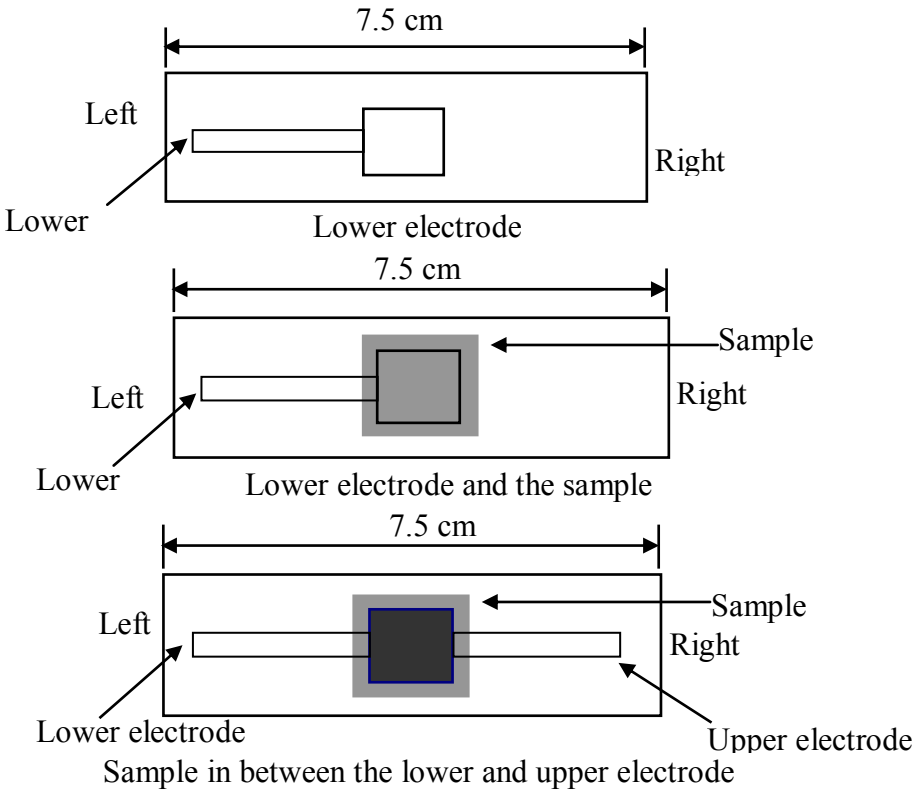

Fig. 3.6: The electrode sample arrangement for the electrical measurement.

The glass substrates were masked with 0.08 m × 0.08 m × 0.001 m engraved brass sheet for the electrode deposition. The electrode assembly used in the study is shown in Fig. 3.6. The glass substrates with mask were supported by a metal rod 0.1 m above the tungsten filament. For the electrode deposition Al was kept on the tungsten filament. The filament was heated by low-tension power supply of the coating unit. The low-tension power supply was able to produce 100 A current at a potential drop of 10 V. During evacuation of the chamber by diffusion pump, the diffusion unit was cooled by the flow of chilled water and its outlet temperature was not allowed to rise above 305 K. When the penning gauge reads about 10^{-5} Torr, the Al on tungsten filament was heated by low-tension power supply until it was melted.

The Al was evaporated, thus lower electrode onto the glass slide was deposited. Al coated glass substrates were taken out from the vacuum coating unit and were

placed on the middle of the lower electrode of the plasma deposition chamber for OMA thin film deposition under optimum condition. The top Al electrode was also prepared on the PPBN film as described above [52-54].

3.7 Measurement of Thickness of the Thin Films

Since the film thicknesses are generally of the order of a wavelength of light, various types of optical interference phenomena have been found to be most useful for measurement of film thicknesses. Multiple-Beam Interferometry technique was employed for the measurement of thickness of the PPBN thin films. This technique is described below.

Multiple-Beam Interferometry method utilizes the resulting interference effects when two silvered surfaces are brought close together and are subjected to optical radiation. This interference technique, which is of great value in studying surface topology in general, may be applied simply and directly to film-thickness determination. When a wedge of small angle is formed between unsilvered glass plates, which are illuminated by monochromatic light, broad fringes are seen arising from interference between the light beams reflected from the glass on the two sides of the air wedge. At points along the wedge where the path difference is an integral and odd number of wavelengths, bright and dark fringes occur respectively. If the glass surfaces of the plates are coated

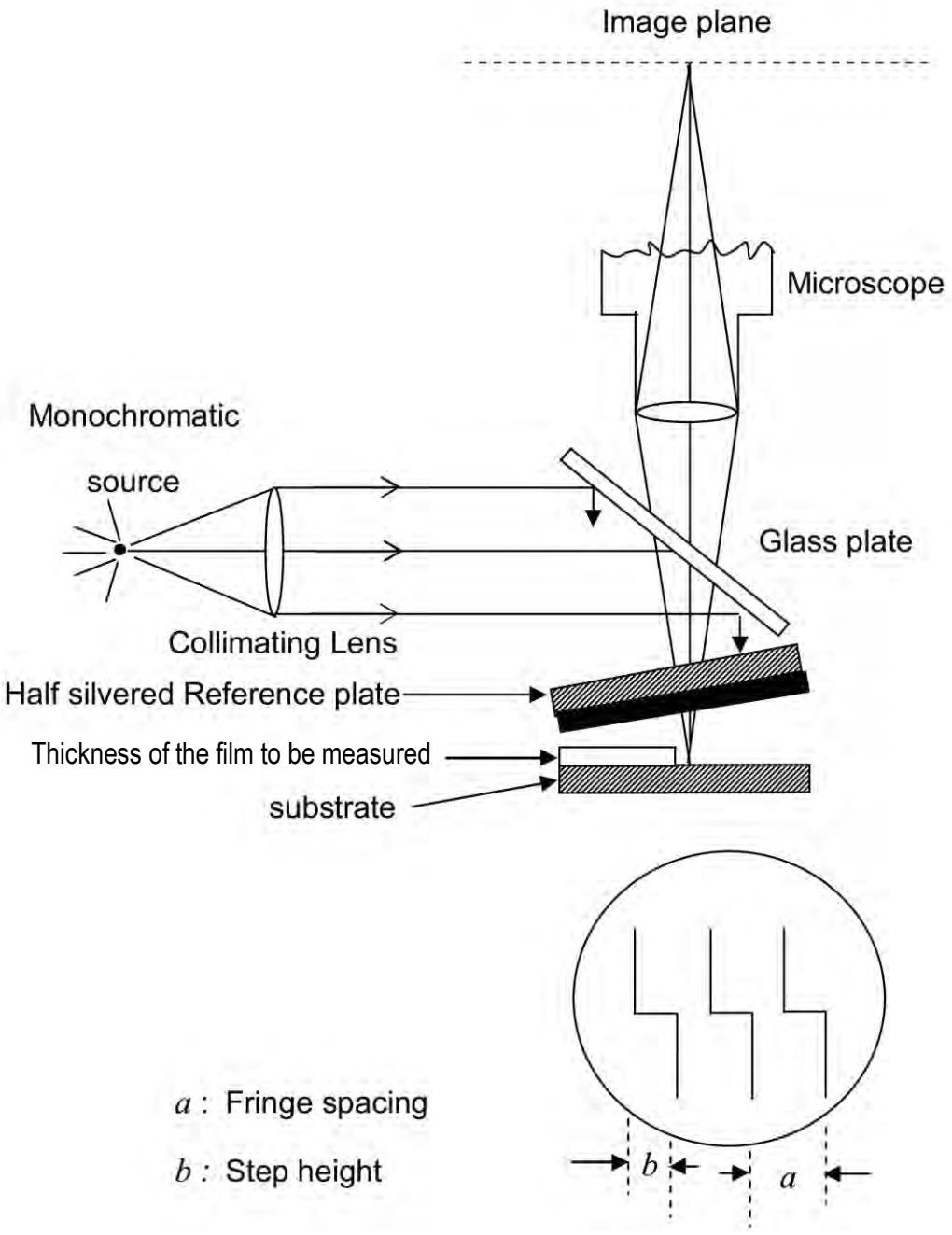

Fig. 3.7: Interferometer arrangement for producing reflection Fizeau fringes of equal thickness.

With highly reflecting layers, one of which is partially transparent, then the reflected fringe system consists of very fine dark lines against a bright background. A schematic diagram of the multiple-beam interferometer along with a typical pattern of Fizeau fringes from a film step is shown in Fig.3.7. As shown in this figure, the film whose thickness is to be measured is over coated with a silver layer to give a good reflecting surface and a half-silvered microscope slide is laid on top of the film whose

thickness is to be determined. A wedge is formed by the two microscope slides, and light multiply reflected between the two silvered surfaces forms an interference pattern with a discontinuity at the film edge as shown in Fig.3.7. The thickness of the film *d* can then be determined by the relation,

$$d = \frac{\lambda}{2}\frac{b}{a}$$

Where, λ is the wavelength and *b/a* is the fractional discontinuity identified in the figure.

In general, the sodium light is used, for which λ = 5893 A°. In conclusion, it might be mentioned that the Tolansky method of film-thickness measurement is the most widely used and in many respects also the most accurate and satisfactory one [56].

3.8 Fourier Transform Infrared Spectroscopy

The Fourier Transform Infrared (FTIR) spectrum of BN was recorded at room temperature by using a double beam IR spectrophotometer (SHIMADZU, FTIR-8900 spectrophotometer, JAPAN) in the wave-number range of 400-4000 cm^{-1}. The FTIR spectrum of the monomer BN was obtained by putting the liquid monomer in a potassium bromide (KBr) measuring cell PPBN powder was collected from the PPBN deposited substrates and then pellets of PPBN powder mixed with KBr were prepared for recording the FTIR spectrum of PPBN sample. The FTIR spectra of the BN and the PPBN were recorded in transmittance (%) mode.

Figure 3.8: The FTIR spectrometer 8900

3.9 Thermal Analyses

Melting and degradation temperatures of the neat PPBN samples were monitored by DTA and thermogravimetric analyzer (TGA) [Seiko-Ex-STAR-6300, Japan]. The measurements using DTA and TGA were carried out from room temperature 300 to 850 K at a heating rate of 20 K/min under nitrogen gas flow. While the DTA traces give the melting and degradation temperatures as determined from the exotherm versus temperature curves, the TGA runs exhibit the weight-loss of the sample with temperature.

3.10 UV-Visible Spectroscopy

The PPBN thin films were deposited on to glass substrates (Sail brand, China) having a dimension of 18mm×18mm×1mm. The UV-Vis spectrum of the monomer (OMA) and the as-deposited and heat-treated PPBN thin films were recorded in absorption mode using a dual beam UV-vis spectrophotometer (SHIMADZU UV-1601, JAPAN) in the wavelength range of 300-900 nm at room temperature.

PPBN thin films were heat-treated for one hour using a furnace, (Muffle Furnace, India). For measuring the optical absorption of the monomer, it was kept in a quart cell and for the PPBN films a similar glass slide was used as the reference.

Figure 3.9 The UV- Visible spectrometer Shimadzu UV-1601

3.11 AC Electrical Measurements

Al/PPBN/Al sandwich structure samples prepared for ac measurements. The measurement was done at fixed temperatures in the temperature 298, 323, 348, 373, 398 and 423 K for the as-deposited PPBN. The ac measurement was performed in the frequency range from 10^1 to 10^6 Hz and temperature range 298-423 K, by a low frequency (LF) Impedance analyzer, Agilent 4192A, 5 Hz - 13 MHz, Agilent Technologies Japan, Ltd.

The temperature was recorded by a Chromel- Alumel thermocouple placed very close to the sample which was connected to a Keithley 197A digital microvoltmeter (DMM). To avoid oxidation, all measurements were performed in a vacuum of about 10^{-2} Torr. Photographs of sample electroding and ac measurement set-up are shown in Figs. 3.10(a) and (b)

(a)

(b)

Fig. 3.10: Photographs of the (a) Sample Chamber (b) the ac electrical measurement set-up.

4.1 Introduction

Plasma polymers have received much attention for their potential applications as light guide material, optical fibers, as photovoltaic energy converters, photodiodes, optical coatings to inhibit corrosion, etc. [62-64]. For these kinds of applications, plasma polymerized thin films need vast thermal, structural and optical investigations. In view to this the thermal, structural and optical properties of the PPBN thin films were studied by DTA, TGA, DTG, FTIR and UV-Visible (UV-vis) spectroscopic analyses and are discussed in this chapter.

As the plasma-polymerized thin films have good dielectric properties, they have been found to be useful as dielectrics in integrated microelectronics and insulating layers for semiconductors, thin film insulators and capacitors in electrical and electronic devices, etc. [63- 64]. Thin films produced through glow discharge are known to have free radicals or polar groups independent of the nature of monomers. Owing to this reason, these polymers are good candidates for the investigation of dielectric properties. Dielectric properties of plasma-polymerized thin films and detail investigation of the ac conductivity provide information about the conduction process, dielectric constant, relaxation process, etc. which are dependent on frequency and temperature. The ac conductivity and dielectric studies of as-deposited PPBN thin films have been discussed in this chapter.

4.2 Differential Thermal, Thermogravimetric and Differential Thermogravimetric Analyses

DTA, TGA and DTG traces of the BN and as deposited PPBN taken at a scan rate of 20 K/min in nitrogen atmosphere are shown in Fig. 4.1 (a) and (b) respectively. The TGA curve exhibits the weight loss of the samples with increasing temperature.

In the DT, TG and DTG trace of BN of Fig. 4.1 (a) it is observed that the thermal stability temperature, Ts of BN is about 378 K. The thermal degradation temperature, T_d i.e. the 50% weight loss is observed at about 414 K. The corresponding DTA and DTG traces showed an endothermic and an exothermic peak respectively at 414 K.

For PPBN in Fig. 4.1 (b) it is observed in the DTA trace that around the temperature of 340 K a transition occurs and the corresponding TGA shows a peak that may be due to the removal of water content. In TGA curve the weight-decrease slowly starts from 311 K followed by a large weight loss from 500 K i.e. the thermal degradation starts from 500 K. This indicates that, the thermal stability temperature, Ts of PPBN is at about 500 K. The TGA trace shows a uniform weight loss up to 500 K and above this temperature the rate of weight loss is comparatively higher but shows uniformity up to the end of the temperature range. The thermal degradation temperature, T_d i.e. the 50% weight loss is not observed for PPBN. The DTA thermogram shows an exothermic broad band which has a maximum around 545 K indicating a gradual change of the thermal properties of PPBN. The weight loss may be due to the loss of non-constitutional or due to hydrogen evolution and low molecular mass hydrocarbon gases. The gradual fall of DTA trace may be a cause of thermal breakdown of PPBN structure and expulsion of oxygen containing compounds. The corresponding DTG trace indicates the same phenomenon by a broad peak.

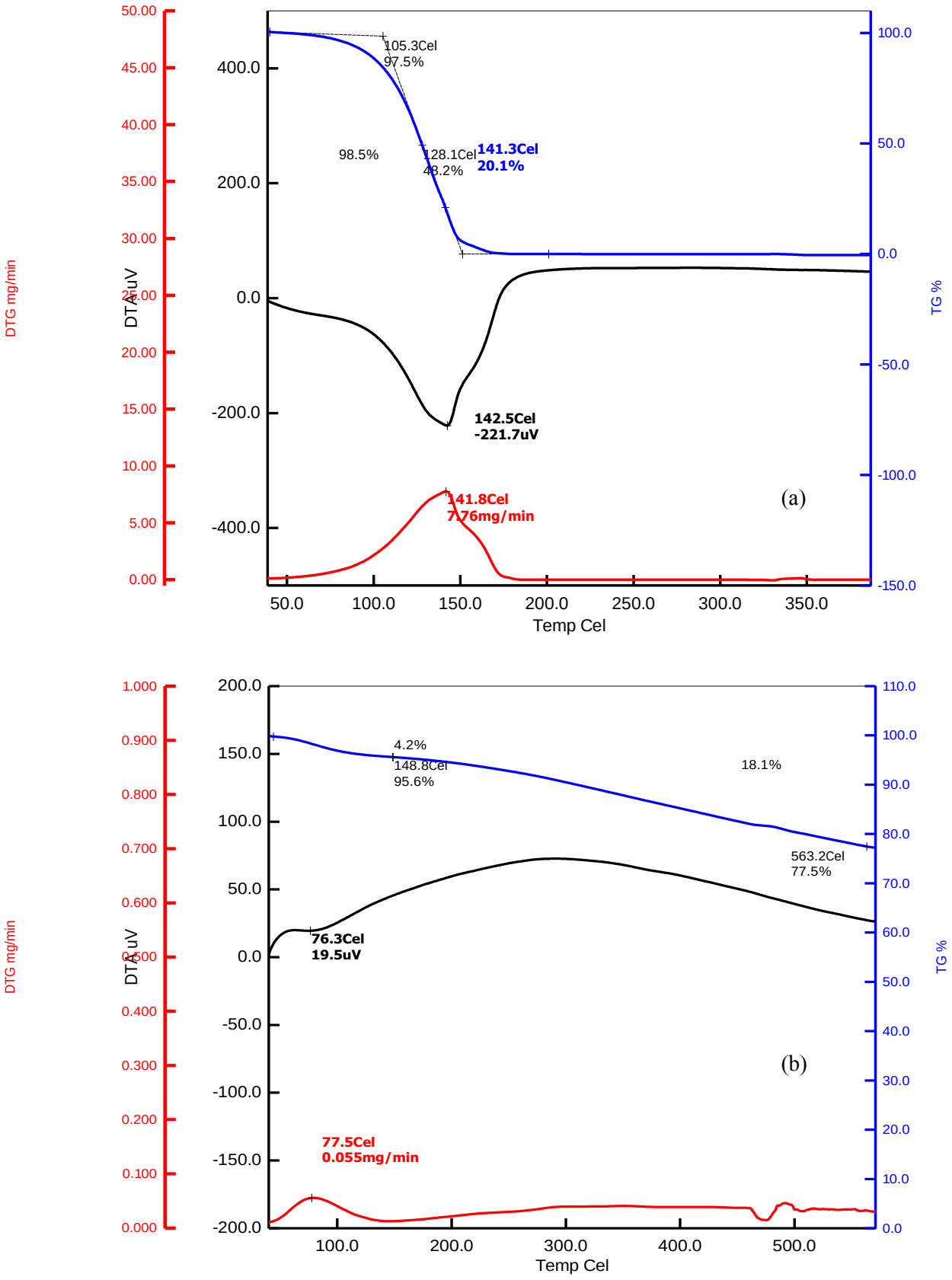

4.1: DTA, TGA and DTG thermograms of (a) BN and (b) as deposited PPBN.

4.3 Fourier Transform Infrared Spectroscopic Analyses

The FTIR spectra of BN and as deposited PPBN are shown in Fig. 4.2. These spectra reveal that the structure of the PPBN thin films deviates to some extent from that of the monomer, BN structure. The absorption bands and their corresponding assignments are listed in Table 4.1.

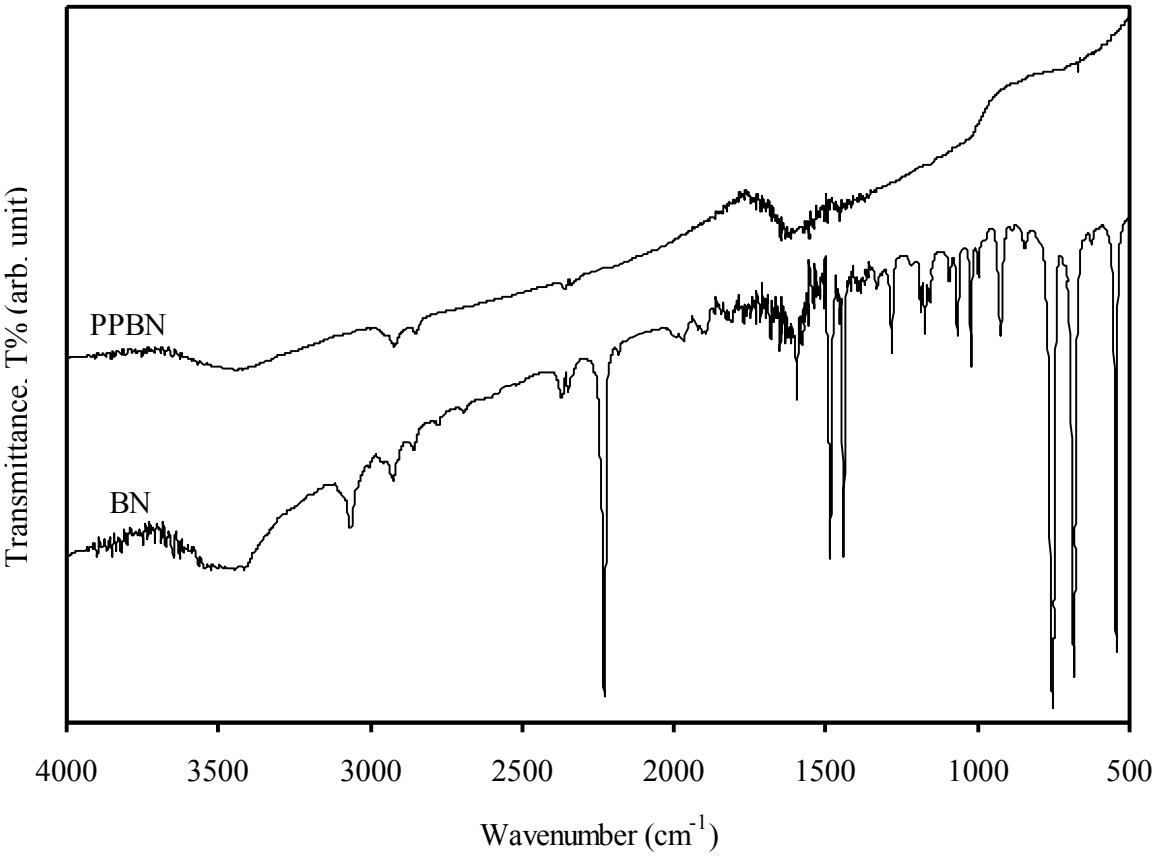

Fig. 4.2: The FTIR spectra of BN and as deposited PPBN.

In Fig. 4.2, spectrum BN shows an extra broad band at 3470 cm^{-1}, which may be due to absorbed water and hydrogen bonded O-H stretching. The peak observed at 3060 cm^{-1} may be due to aromatic C-H stretching and peak at 2920 indicates alkyl C-H stretching vibration and at 2850 cm^{-1} indicates aliphatic C-H stretching vibration. The C≡N stretching vibration is found at 2230 cm^{-1}. The overtone bands for the substitution of benzene ring are found in 1890-1970 cm^{-1}. Absorption peak at 1595 cm^{-1} indicates C=N stretching vibration.

The peaks at 1489 and 1443 cm^{-1} can be assigned as aromatic C=C bonds. The absorption peaks at 1287 cm^{-1} corresponds to the C-H twisting and peak at 1175 cm^{-1} corresponds to the C-N stretching. Peaks at 1068 and 1021 cm^{-1} indicate C-O stretching vibration. Bands at 910 and 842 cm^{-1} are observed due to C-H rocking. The absorption peak at 926 cm^{-1} is found for C-H bending. The strong absorption peak at 753 cm^{-1} confirms the monosubstitution of the benzene ring. Another strong absorption peak at 683 cm^{-1} indicates the aromatic C-N nonplanar bending vibration. The C-C=N deformation vibration at 545 cm^{-1} is observed in BN.

In the spectrum PPBN the absorption band at 3430 cm^{-1} may arise due to O-H stretching vibration, which is similar to that in BN. No band for C-H aromatic stretching observed at 2920 cm^{-1}. Two absorption bands corresponding to aliphatic C-H stretching vibrations are observed at 2910 and 2850 cm^{-1} which are also observed in BN. The overtone bands for the substitution of benzene ring are also found in PPBN. The observed absorption peak at 1595 cm^{-1} for C=N stretching is found as that of BN. The peaks for aromatic C=C bands at 1560 and 1455 cm^{-1} are retained in PPBN [65]. The C-C=N deformation vibration at 545 cm^{-1} are also observed in the PPBN spectrum, indicating that a certain amount of C≡N bonds broke due to plasma and formed C-C=N. The peaks for C-H stretching, C≡N stretching, C-H twisting, C-N stretching, C-O stretching, C-H rocking and C-H bending as observed in BN, is not observed in PPBN, indicating breaking of these bonds. A combination broad absorption peak from 739 to 521 cm^{-1} have arisen due to the presence of monosubstitution of the benzene ring, aromatic C-N nonplanar bending vibration and C-C=N deformation vibration indicating partial breaking of these bonds [66].

Thus, it is found that the chemical nature of the PPBN thin films deposited by plasma polymerization technique does not match to that of the monomer BN. However these observations indicate that the aromatic ring structure is retained in the PPBN thin films. It is seen from the FTIR spectrum of the PPBN thin films that the sharpness of the absorption bands decreases significantly compared to that of BN. This is an indication of monomer fragmentation during plasma polymerization.

Table 4.1: Assignments of IR absorption bands for BN and PPBN.

Assignments	**Wavenumber (cm^{-1})**	
	BN	PPBN
O-H stretching	3470	3430
Aromatic C-H stretching	3060	-
Alkyl C-H stretching	2920	-
Aliphatic C-H stretching	2850	2910, 2850
C≡N stretching	2230	-
Overtone bands	1890-1970	1890-1970
C=N stretching	1595	1595
Aromatic C=C	1489, 1443	1560, 1455
C-H twisting	1287	-
C-N stretching	1175	-
C-O stretching	1068, 1021	-
C-H rocking	910, 842	-
C-H bending	926	-
Monosubstitution of the benzene ring	753	739-521 Merged in Broad band
Aromatic C-N nonplanar bending vibration	683	739-521 Merged in Broad band
C-C=N deformation vibration	545	739-521 Merged in Broad band

4.4 Ultraviolet-visible spectroscopic analyses

The wavelength of light that a compound absorbs is the characteristic of its chemical structure. Specific regions of the electromagnetic spectrum are absorbed by exciting specific types of molecular and atomic motion to higher energy levels. Absorption of ultraviolet and visible radiation is associated with excitation of electrons, in both atoms and molecules, to higher energy states. Most molecules require very high energy radiation. Light in the UV-visible (UV-Vis) region is adequate for molecules containing conjugated electron systems and as the degree of conjugation increases, the spectrum shifts to lower energy.

Amorphous films have a random network in contrast to the crystalline structure. In these materials no long range order is present. The disorder associated with the deficiency of long range order in these materials introduces a high density of localized

electronic states in the band gap which influence the electronic properties of the material.

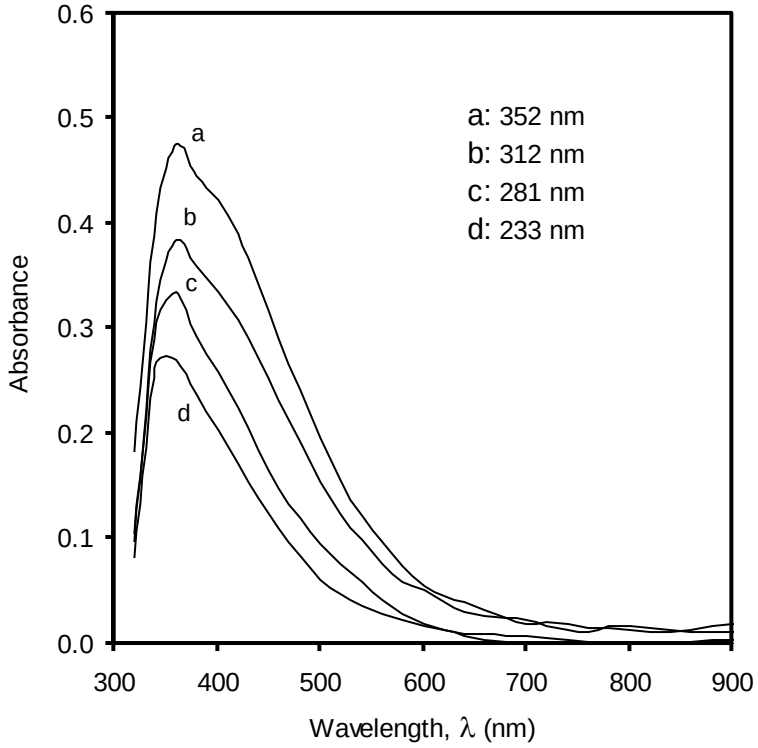

Fig. 4.3: Wavelength, λ versus absorbance plot for PPBN thin films of different thicknesses.

Fig. 4.3 shows the UV-vis spectral behavior of as deposited PPBN thin films for various thicknesses at room temperature (300 K). It is seen that the absorbance increases with the increase of thickness of the PPBN thin films which is due to increased scattering losses. It is observed that the absorbance attains its maximum value around 352 nm and then decreases exponentially as wavelength decreases. The absorption coefficient, α is calculated from the measured absorbance data of Fig. 4.4 for different wavelengths corresponding to different photon energies at room temperature using equation (2.5). Each of the spectrums shows a hump/shoulder in the wavelength region from 400 to 380 nm. This shoulder may have arisen due to the formation of conjugation to some extent in the PPBN thin film structure.

The spectral dependence of α on the photon energy, hν, for all the as deposited PPBN thin films is presented in Fig. 4.4. The dependence of optical absorption coefficient, α on the photon energy, hν helps to study the band structure and the type of transition of electrons. The absorption edge starts increasing around 1.6 eV and there is a rapid rise

of α from 2.2 eV. From the plot it is clear that the curves have different slopes indicating the presence of different optical transitions in the PPBN thin films.

From UV-vis spectra optical band gap and nature of the induced optical transitions were determined. In crystalline and amorphous materials the photon absorption is observed to obey the Tauc relation, equation (2.8).

The indirect transition energy gap (E_{gi}) can be obtained by plotting $(\alpha h\nu)^{1/2}$ versus hν curve and then extrapolating the linear portion of the curve to $(\alpha h\nu)^{1/2} = 0$. Also from the plots of $(\alpha h\nu)^2$ versus hν, direct transition energy gap (E_{gd}) can be determined by extrapolating the linear portion of the plots to the intercept in the *hν* axis [54].

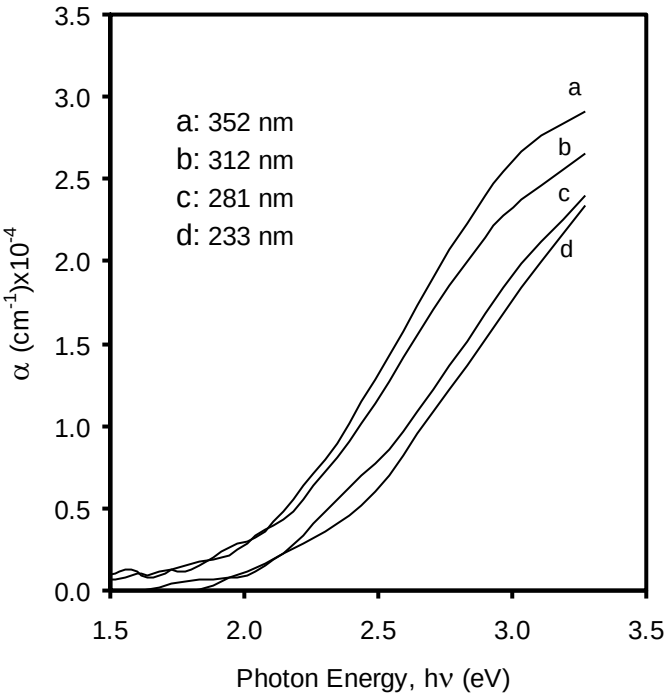

Fig. 4.4: Photon energy versus absorption coefficient (α) plot for PPBN thin films of different thicknesses.

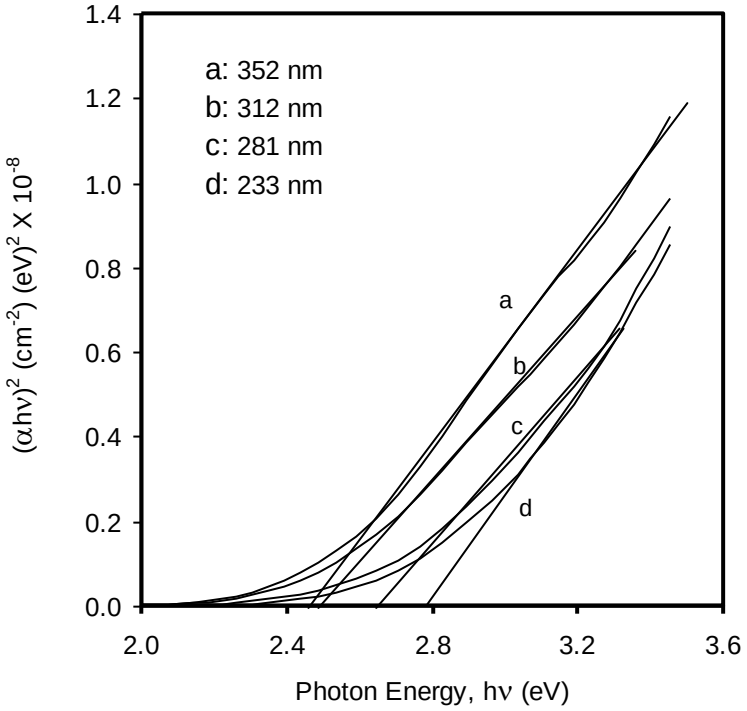

Fig. 4.5: $(\alpha h\nu)^2$ versus hν curves for as deposited PPBN thin films of different thicknesses.

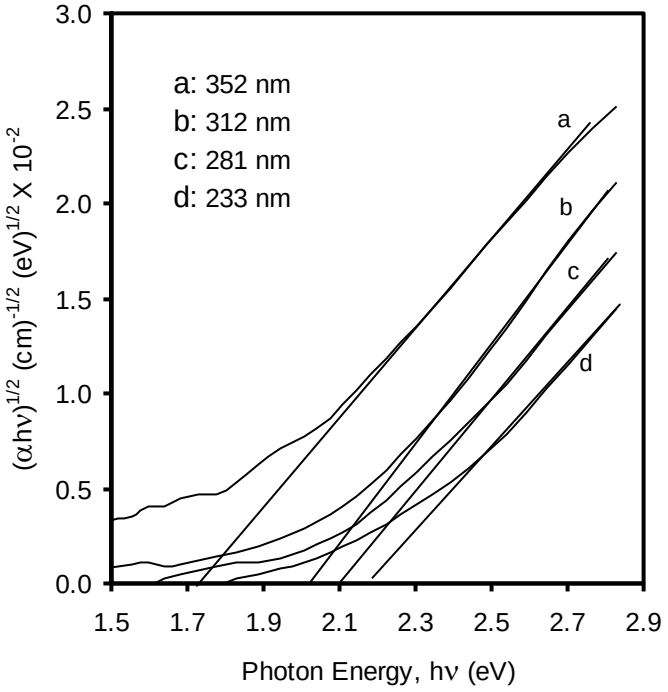

Fig. 4.6: $(\alpha h\nu)^{1/2}$ versus hν curves for as deposited PPBN thin films of different thicknesses.

Table 4.2: Values of direct and indirect band gap energies.

Film thickness d (nm)	Direct band gap E_{gd} (eV)	Indirect band gap E_{gi} (eV)
233	2.80	2.20

281	2.66	2.10
312	2.51	2.03
352	2.47	1.73

$(\alpha h\nu)^2$ as a function of hν is plotted in Fig. 4.5 and $(\alpha h\nu)^{1/2}$ as a function of hν is plotted in Fig. 4.6 to obtain the E_{gi} and E_{gd} of the as deposited PPBN thin films respectively. The E_{gi} and E_{gd} of the as deposited PPBN thin films are determined from the intercept of the linear part of the curves extrapolated to zero α in the photon energy axis. The values of the E_{gi} and E_{gd} for as deposited PPBN thin films are recorded in Table 4.2. The values of E_{gd} varies from 2.80 to 2.47 eV, and those of E_{gi} varies from 2.20 to 1.73 eV as the thickness varies from 233 to 352 nm for as-deposited PPBN thin films. It is observed that the values of E_{gd} and E_{gi} for as deposited PPBN thin films have a decreasing trend with the increase of film thicknesses. As the thickness of the films increases, some crosslinking may develop within the bulk of the material with increasing deposition time and as a consequence lower energy gaps are observed. The decrease in E_g with increasing thickness is attributed due to the merge of defect states at the top and bottom of the valance band and conduction band respectively.

4.5 Alternating Current Electrical Properties

The ac conductivity ($\sigma_{ac)}$ and dielectric relaxation processes of plasma-polymerized thin films provide information regarding the conduction mechanism and relaxation processes. For this, detail investigation of the σ_{ac} and dielectric properties of PPBN thin films which are dependent on frequency and temperature, are discussed in the subsequent sections.

4.5.1 Frequency and temperature dependence of ac electrical conductivity

The σ_{ac} as a function of frequency in the frequency range 10^3 to 10^6 Hz for PPBN thin films of different thicknesses at the room temperature is shown in Fig 4.7 and at different temperatures of 298, 323, 348, 373 and 398 K are shown in Fig. 4.8 to 4.10.
It is observed that ζ_{ac} increases linearly with the frequency of the applied signal with higher slope in the lower frequency region and lower slope in the high frequency region (f >100 kHz) for all the measurement temperatures. It is also clear that the

variation in the logarithmic ac conductivity is almost linear with the variation in logarithmic frequency and that $\zeta_{ac}(\omega)$, increases with increasing frequency.

The variation of ζ_{ac} with frequency can be expressed by the relation $\sigma_{ac}(\omega) = A\omega^n$. where $\omega = 2\pi f$ is the angular frequency and n is an index which is used to determine the possible conduction or relaxation mechanism operative in amorphous materials.

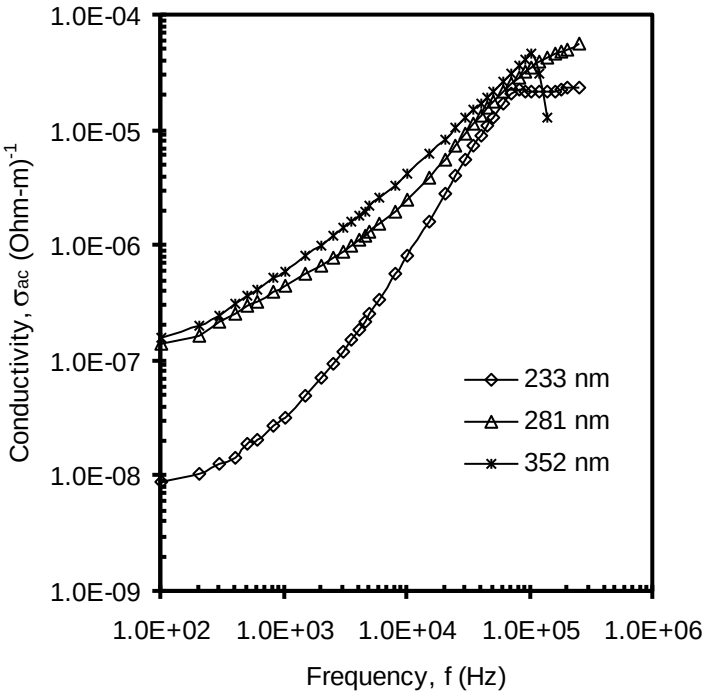

Fig.4.7 Dependence of ac conductivity, ζ_{ac}, on frequency at room temperature for PPBN thin films of different thicknesses.

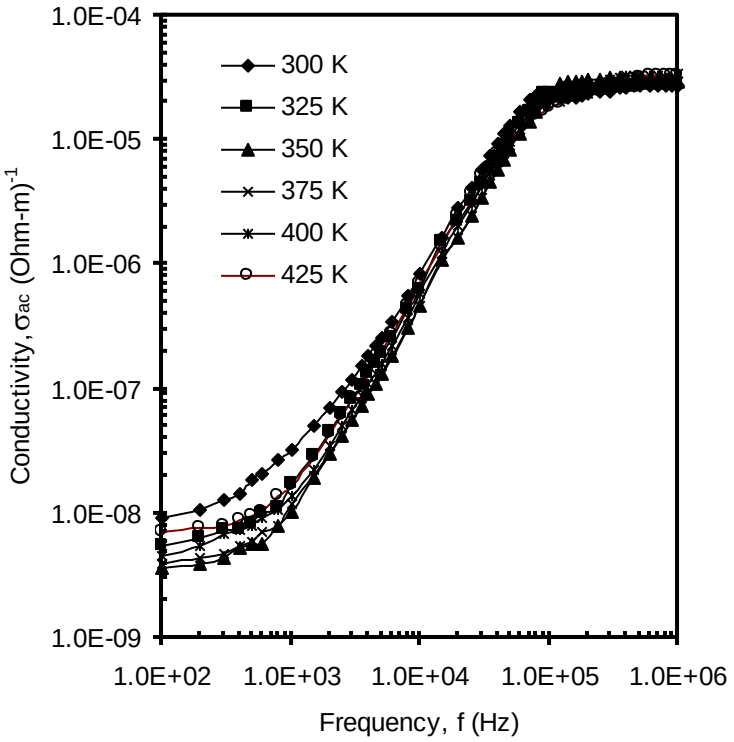

Fig.4.8 Dependence of ac conductivity, ζ_{ac}, on frequency at different temperatures for PPBN thin film of thickness 233 nm.

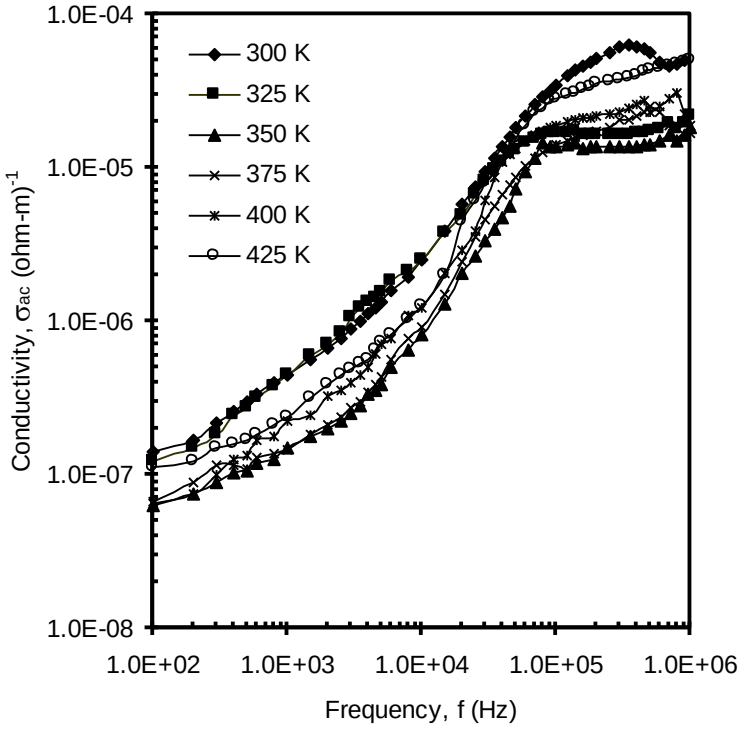

Fig.4.9 Dependence of ac conductivity, ζ_{ac}, on frequency at different temperatures for PPBN thin film of thickness 281 nm.

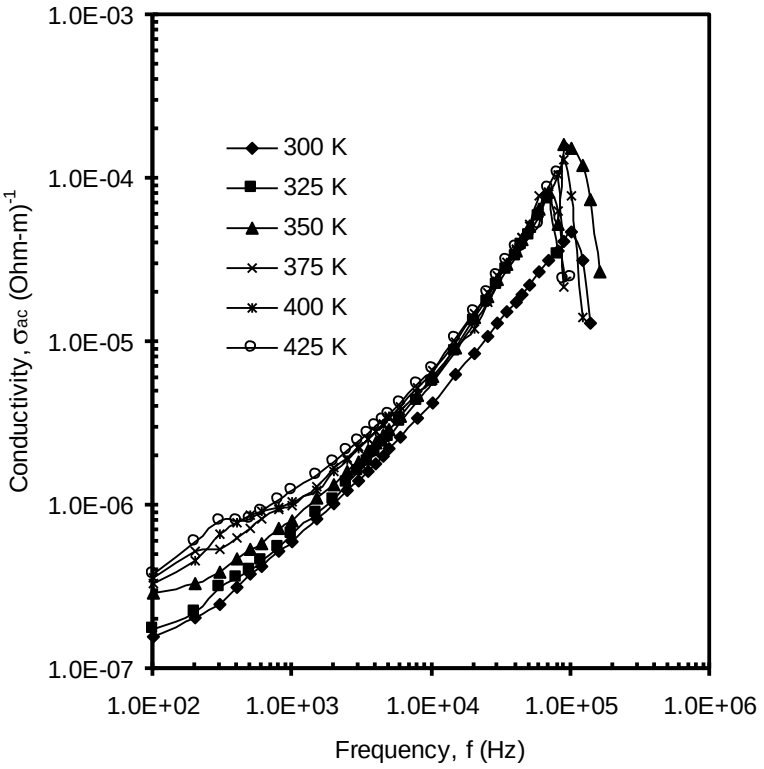

Fig.4.10 Dependence of ac conductivity, ζ_{ac}, on frequency at different temperatures for PPBN thin film of thickness 352 nm.

The values of the exponent „n" for as deposited PPBN thin films were calculated to be about 0.24 to 0.89 in the low frequency (10 Hz-10^4 Hz) region and 1.02 to 1.77 in the high frequency region (above 10^4 Hz) in all the five measurement temperatures and are tabulated in Table 4.3. The exponent n is the measure of departure from ideal Debye type of relaxation process. It has been shown that when $n \leq 1$ the polarization process is of Debye-type (the case of nearest-neighbour interacting dipoles). The calculated values of the frequency exponent, n of PPBN thin films correspond to Debye-type in the lower frequency region and in the high frequency region correspond to the relaxation process other than Debye type. The σ_{ac} curve shows that σ_{ac} is very sensitive to the frequency both in the low and intermediate frequencies except for the dispersion process in the high frequencies. It is also observed from Fig 4.7 that the σ_{ac} increases with increasing thickness. As, the plasma polymerized thin films are known to have free radicals and have a tendency to react with O, the

increase in ζ_{ac} may be dominated by the increased density of free radicals reacting with O with increasing thickness.

Table 4.3: Values of „n" in $\sigma_{ac}(\omega) = A\omega^n$ of PPBN thin films of different thicknesses.

Frequency f (Hz)	Temperature T (K)	Values of „n"		
		Thickness d ± 5 (nm)		
		233	281	352
Low 10^2-10^3 Hz	300	0.70	0.89	0.60
	325	0.74	0.58	0.63
	350	0.64	0.62	0.27
	375	0.53	0.57	0.24
	400	0.57	0.54	0.53
	425	0.31	0.67	0.41
High $>10^3$ Hz	300	1.04	1.60	1.24
	325	1.36	1.65	1.02
	350	1.40	1.73	1.56
	375	1.58	1.38	1.23
	400	1.08	1.60	1.02
	425	1.45	1.31	1.77

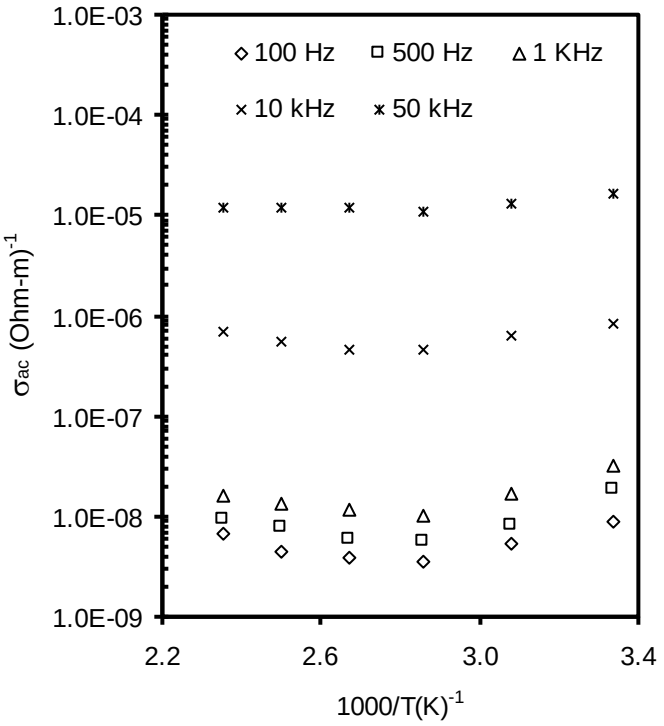

Fig. 4.11 Dependence of ac conductivity, $\zeta_{ac,}$ on temperature at different frequencies for PPBN thin film of thickness 233 nm.

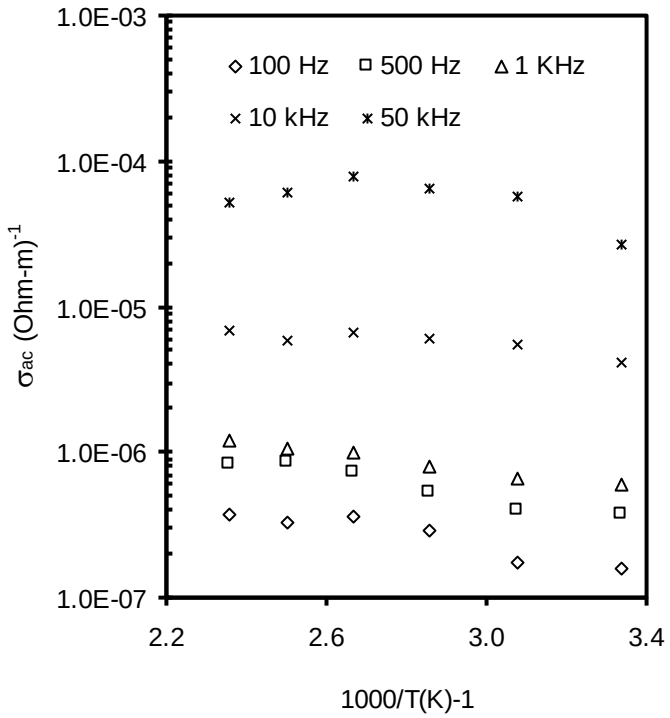

Fig. 4.12 Depdenceof ac conductivity, $\zeta_{ac,}$ on temperature at different frequencies for PPBN thin film of thickness 281 nm.

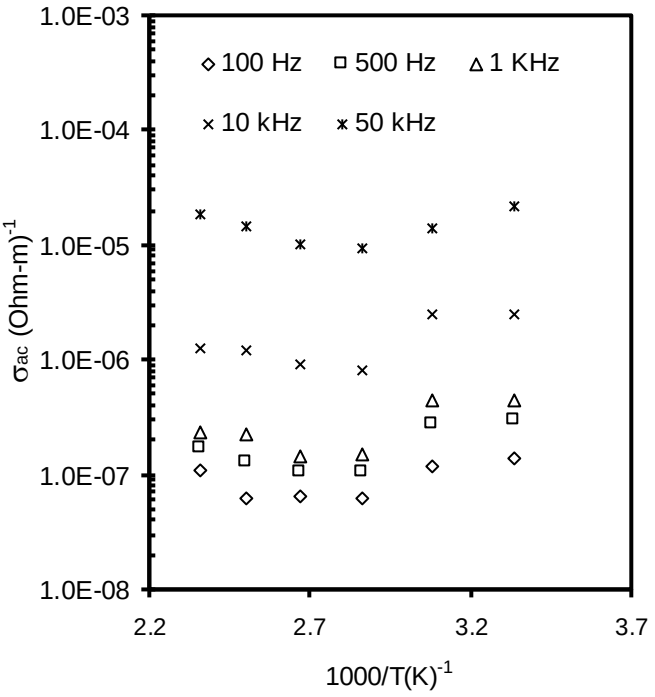

Fig. 4.13 Dependence ac conductivity, $\zeta_{ac,}$ on temperature at different frequencies for PPBN thin film of thickness 352 nm.

Figs. 4.10 to 4.13 show the variation of σ_{ac} as a function of reciprocal temperature at different frequencies for PPBN thin films of different thicknesses. From the plots shown in Figs. 4.10 to 4.13 the activation energies, ΔE for carrier conduction were calculated and it is found that the values ΔE of have a very small value (~ 0.050 eV). The low value of the ΔE and the increase of ζ_{ac} (ω), with the increase of frequency confirm that hopping conduction is the dominant current transport mechanism in PPBN thin films.

4.5.2 Frequency and temperature dependence of the dielectric constant

The dependence of dielectric constant (ε′) on frequency can be expressed by the well known Debye dispersion formula (equation 2.16) which expresses the complex permittivity related to the free dipoles oscillating in an alternating electric field.

At very low frequencies ($\omega << 1/\tau$), dipoles follow the field and then $\varepsilon^{/} = \varepsilon_s$. As the frequency increases dipoles begin to "lag" behind the field and $\varepsilon^{/}$ slightly decreases. This nature of ε' is observed in PPBN thin films. When frequency reaches the characteristic frequency ($\omega = 1/\tau$) the dielectric constant drops abruptly. At very high

frequencies ($\omega >> 1/\tau$) the dipoles can no longer follow the field and $\varepsilon' \approx \varepsilon_\infty$ can be observed.

The capacitance measurement was performed in the frequency range 100 Hz to 1 MHz at temperatures 300, 325, 350, 375, 400 and 425 K.

Figs. 4.15 to 4.17 show the dependence of ε′ on frequency at different temperatures for PPBN thin films of different thicknesses. It can be seen from this figure that the ε' decreases slowly with the increase of frequency in the low frequency region and after a particular frequency it drops sharply and approaches a constant value at higher frequencies. This phenomenon indicates space charge or interfacial polarization at low frequency and dipolar polarization at higher frequency region. It is also observed that for a particular frequency the ε' is decreased from its initial value with the increase in sample temperature. The value of the ε' of PPBN thin films of different thicknesses is found to vary between 8.6 and 23.6 at different temperatures in the low frequency region (<10 kHz). The general trend of ε' is to decrease with increasing temperature and this trend is also observed in all as-deposited PPDBN thin films in the temperature range from 300 to 425 K. In low frequency the temperature dependence of the ε' reflects the temperature dependence of the ε_0. In PPBN thin films the lesser dependence of ε' on temperature in the high frequency region and the higher dependence of ε' on temperature in the low frequency region may be attributed to the thermal expansion of the polymer which causes the decrease of ε'.

It is also observed in Fig. 4.14 that ε' of the PPBN increases as the film thickness increases. The presence of absorbed moisture and/or C=O and polar group density probably increase with the increasing thickness of PPBN thin films due to the presence of more dangling bonds and hence increases the ε' with increasing thickness.

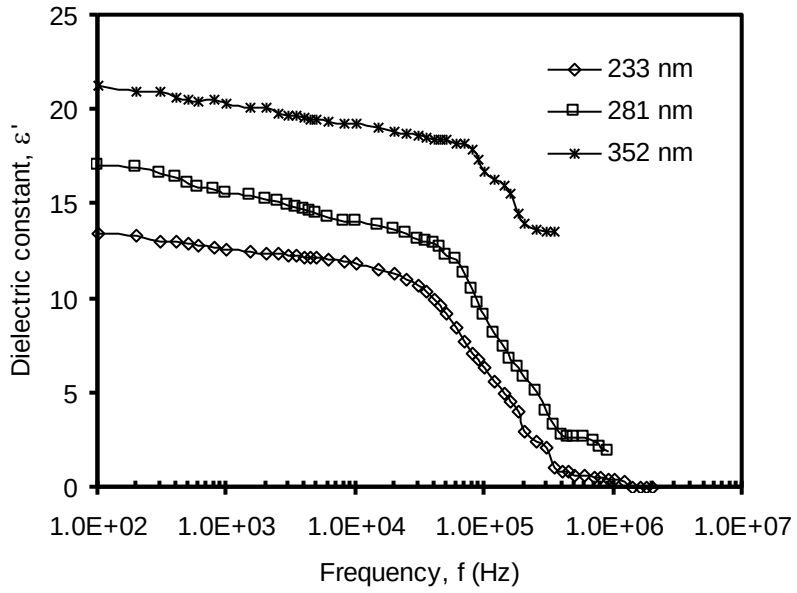

Fig 4.14 Variation of dielectric constant with frequency at room temperature for PPBN thin films of different thicknesses.

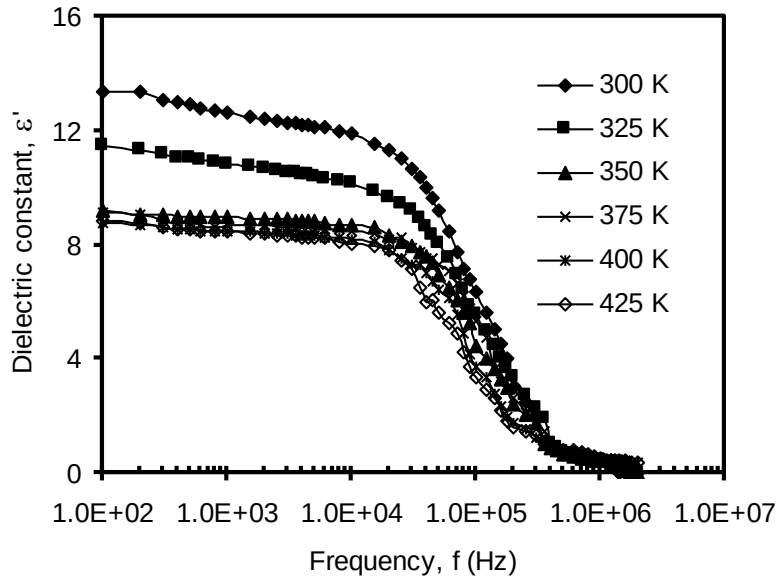

Fig. 4.15 Variation of dielectric constant with frequency at different temperatures for PPBN thin film of thickness 233 nm.

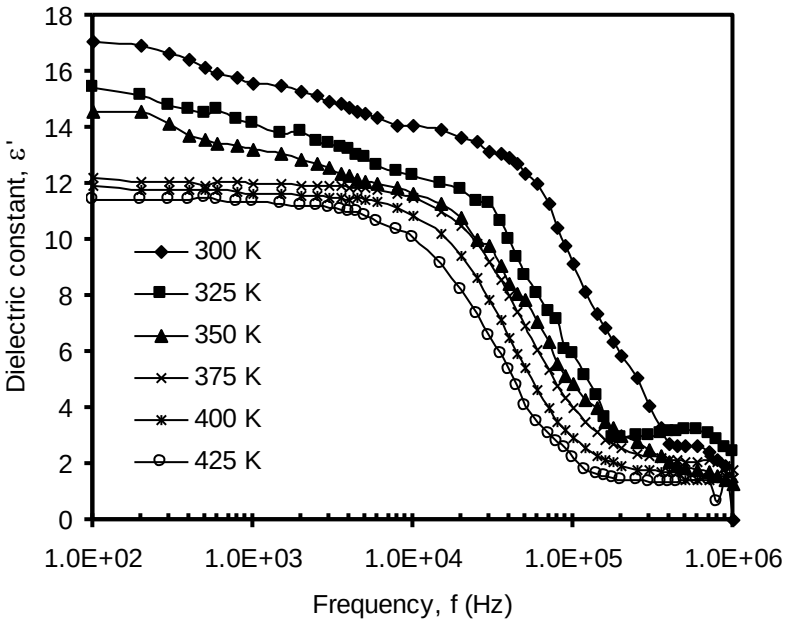

Fig.4.16 Variation of dielectric constant with frequency at different temperatures for PPBN thin film of thickness 281 nm.

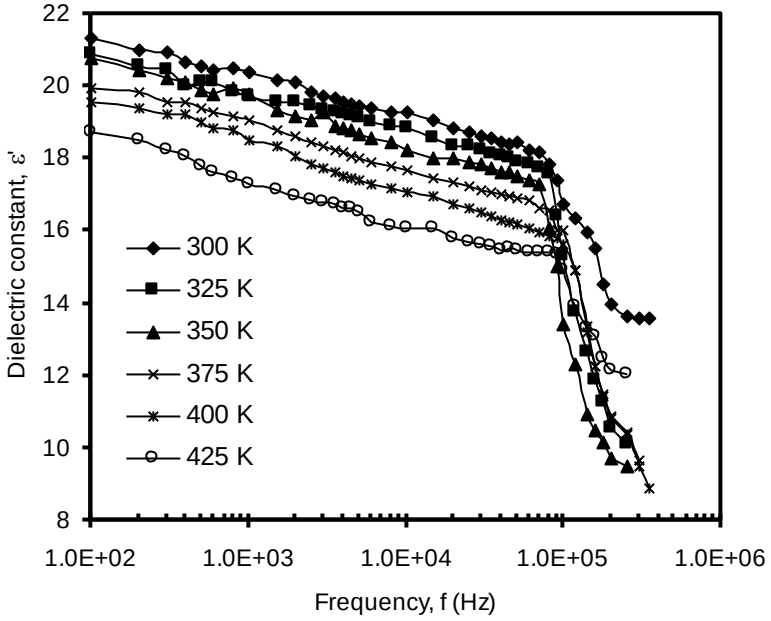

Fig.4.17 Variation of dielectric constant with frequency at different temperatures for PPBN thin film of thickness 352 nm.

4.5.3 Frequency and temperature dependence of dielectric loss tangent

The variation of loss tangent with frequency for PPBN thin films of different thicknesses at different temperatures are depicted in Fig. 4.18 to 4.20. It is observed from the plots that in the low frequency region *tanδ* decreases as the frequency increases followed by a loss minimum. This phenomenon is usually associated with ion drift or interfacial polarization involving ionic movement. After that the *tanδ* increases with the increase in frequency and attains a peak at around 10^5 Hz and then decreases. This phenomenon is also evident in the decrease of ε', as the dipole orientation can not keep up at high frequency. It is also observed that similar peaks are present at the higher temperatures with a slight shift in the peak position. In the low frequency region *tanδ* shows a loss minimum in the frequency range from 100-1000 Hz i.e. a low frequency relaxation process and the loss shifts toward higher frequency side with increasing temperature. In PPBN thin films the maximum value of *tanδ* have not shown any definite trend in the lower temperature region (300 to 350 K) which may be due to the evolution of small amount of absorbed moisture in PPBN thin films. Whereas, in higher temperature region (375 to 425 K) the maximum value of *tanδ* increases with increasing temperature i.e. charge carriers increase by thermal activation at higher temperature.

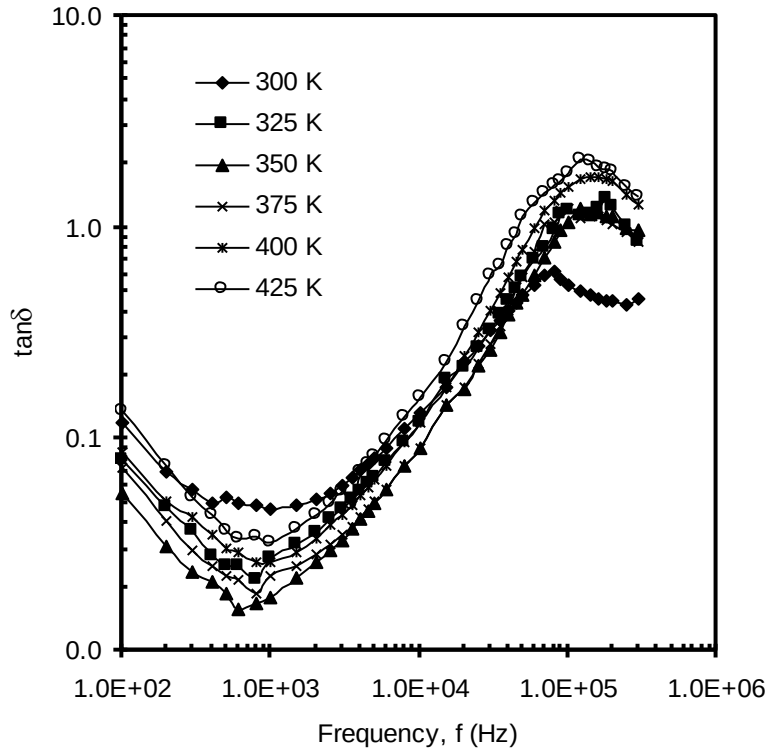

Fig. 4.18 Dependence of loss tangent, tanδ, on frequency at different temperatures for PPBN thin film of thickness 233 nm.

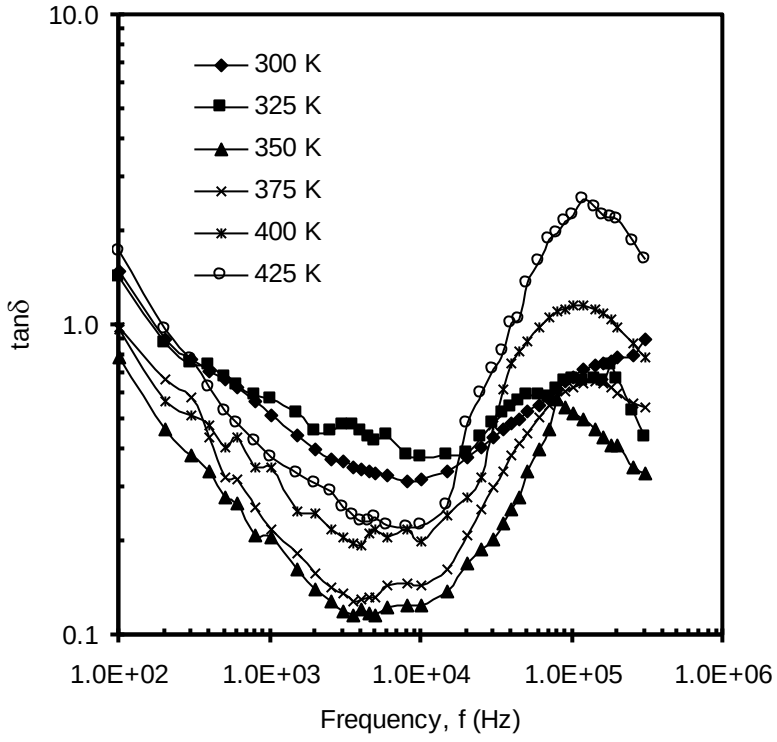

Fig.4.19 Dependence of loss tangent, tanδ, on frequency at different temperatures for PPBN thin film of thickness 281 nm.

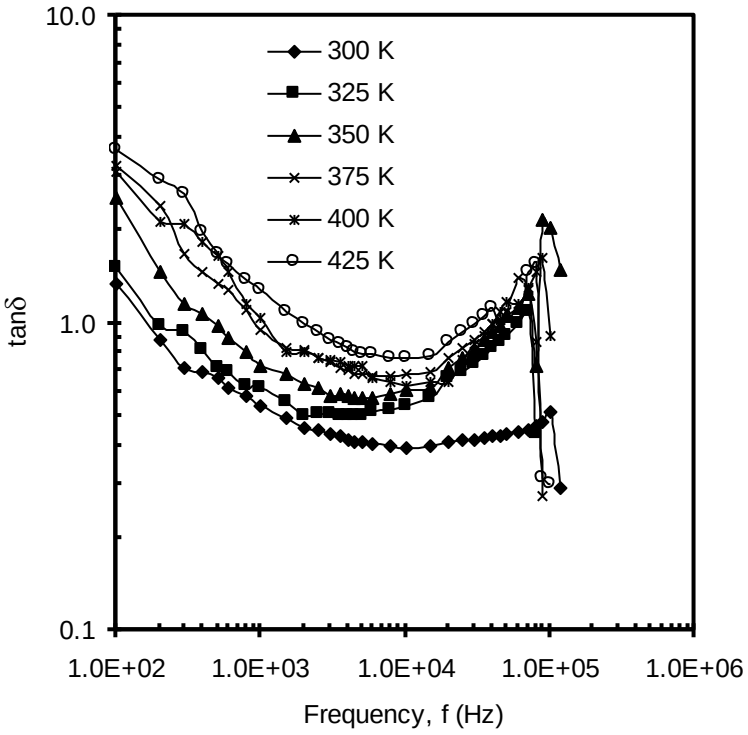

Fig. 4.20 Dependence of loss tangent, tanδ, on frequency at different temperatures for PPBN thin film of thickness 352 nm.

5.1 Conclusions

Capacitively coupled Plasma polymerized method was used to get Plasma polymerized Benzonitrile (PPBN) thin films of different thickness under glow discharge plasma. The optical and frequency and temperature dependence of ac electrical properties along with structural and thermal properties of the PPBN thin films were studied. The results can be concluded as follows:

The TGA trace showed a transition in a particular temperature where the DTA showed a peak which may be due to the removal of water content and the break of bonds in the monomer. The gradual fall of DTA may be a cause of thermal breakdown of PPBN structure and expulsion of oxygen containing compounds. The thermal stability temperature, Ts of BN and PPBN are about 378 and 500 K respectively.

It is seen from the FTIR spectrum of PPBN thin film that the sharpness of the absorption bands decreases significantly compared to that of the monomer spectrum. This is an indication of monomer fragmentation during plasma polymerization. In the FTIR spectrum of PPBN there are some absorption bands similar to that of BN but with significant decrease in absorption with slight shifting in position, which indicate that the chemical nature of the PPBN thin films deposited by plasma polymerization technique is different from that of BN.

As the thickness of the films increases electronic transition occurs from the more depth of the samples which need more energy. It is found that the peak wavelength shifts to lower wavelength for PPBN thin films with increase in thickness. The dependence of optical absorption coefficient on the photon energy indicates that the absorption edge starts increasing around 1.6 eV and there is a rapid rise in absorption coefficient from 2.2 eV. The values of E_{gd} varies from 2.80 to 2.47 eV, and those of E_{gi} varies from 2.20 to 1.73 eV as the thickness varies from 233 to 352 nm for PPBN thin films. It is observed that the values of E_{gd} and E_{gi} for as deposited PPBN thin films have a decreasing trend with the increase of film thicknesses. As the thickness of the films increases, some fragmentation/crosslinking may develop within the bulk of the material with increasing deposition time and as a consequence lower energy gaps are observed. The decrease in E_g with increasing thickness is assumed to appear due to the merge of defect states and generation of sublevels at the end of the valance band and conduction band.

It is found that (σ_{ac}) increases linearly with the frequency of the applied signal with different slopes. The values of the exponent ‘n’ for as deposited PPBN thin films were

calculated to be around 0.24 to 0.89 in the lower frequency region (10 Hz-10^4 Hz) and 1.02 to 1.77 in the higher frequency region (above 10^4 Hz). The calculated values of the frequency exponent, *n* of PPBN thin films correspond to Debye-type in the lower frequency region and in the high frequency region correspond to the relaxation process other than Debye type. It is found that the activation energies, ΔE for carrier conduction have a very small value (~ 0.050 eV). The low value of the ac activation energy and the increase of $\sigma_{ac}(\omega)$, with the increase of frequency confirms that hopping conduction is the dominant current transport mechanism in PPBN films.

The frequency dependent dielectric constant of PPBN films of different thickness showed that for all the samples ε' remains almost constant up to a particular frequency and then starts to decrease sharply. It is observed that ε' decreases slowly with increasing frequency which indicates space charge or interfacial polarization at low frequency and dipolar polarization at higher frequency region. It is also observed that for a particular frequency the ε' is decreased from its initial value with the increase in sample temperature. The value of the ε' of PPBN thin films of different thicknesses is found to lie between 8.6 and 23.6 at different temperatures in the low frequency region (<10 kHz). It is also observed that ε' of the PPBN increases as the films thickness increases. From the variation of loss tangent, tanδ with frequency at room temperature for different samples it is noticed that tanδ increases with the increase in frequency having a peak around 10^5 Hz. It is observed that similar peaks are present at all the PPBN films of different thickness. It is also observed that similar peaks are present at the higher temperatures with a slight shift in the peak position.

5.2 Suggestions for Further Work

The morphological, structural, thermal, optical and ac electrical behavior of as deposited PPBN thin films are investigated in the present work. More investigations are needed to explain different characteristics elaborately, which will help finding suitable application of this material. The following investigations may be carried out for further study.

The direct current electrical properties can be carried out for the PPBN thin films in different conditions. The dependence of current density on the applied voltage at different temperatures in samples of different thicknesses can be studied. These investigations can help to identify the dominant charge conduction mechanism operative under dc field in PPBN thin films.

To observe the nature and source of the radicals in PPBN films, electron spin resonance (ESR) study may be carried out.

PPBN can be modified to change the electrical properties by heat treatment and doping. Doping of thin films can be introduced during the preparation of the films in plasma chamber or by exposing them in the dopant gases.

For studying the charge storage and charge relaxation the thermally stimulated depolarization current (TSDC) can be measured.

The PPBN thin films can be also deposited as a coating on other polymers rather than on glass substrate. These films can also be prepared in an asymmetric electrode configuration or using inductively coupled plasma polymerization set up with rf power and can be characterized by the above mentioned techniques.

References

[1] D"Agostino, R. Ed. "Plasma Deposition Treatment and Etching of polymers", Academic Press, San Diego, (1990).

[2] Zhao, X. Y., Wang, M. Z. and Xiao J., "Deposition of plasma conjugated polynitrile thin films and their optical properties", Euro. Polym J.,vol 42, 2161-2167, (2006).

[3] Kim, M. C., Cho, S. H., Lee, S. B., Kim, Y. and Boo, J. H., "RF-plasma polymerization and characterization of Polyaniline", Thin Solid Films, vol 447-448, 592-598, (2004).

[4] Mathai, C. J., Saravanan, S., Anantharaman, M. R., Venkitachalam, Jayalekshmi, S., "Characterization of low dielectric constant polyaniline thin film synthesized by ac plasma polymerization technique", J. Phys. D Appl. Phys., vol 35, 240-245, (2002).

[5] S. R. Forrest, IEEE journal on selected topics in Quantum Electronics, 6(6) (2000)1072-1083.

[6] Frank F .Shi, "Developments in plasma –polymerized organic thin films with novel mechanical, electrical and optical properties" J.M.S-Rev. Macromal Chem.Phys., 36(4)(1996) 795-826.

[7] Yasuda, H., "Plasma polymerization" Academic Press; Orlando, (1985).

[8] A T., Bell and M., Shen (Eds), "Plasma Polymerization" Am. Chem. Soc., Washington, D.C. (1979).

[9] Agostino, R.d", Ed., "Plasma deposition, treatment, and etching of polymers" Academic Press, Boston (1990).

[10] Suhr, H. and Bell A. T., "In Technique and application of plasma chemistry: Hollahan", Ed.; John wilcy & Sons, New York (1974).

[11] Biederman, H. and Slavinska, D., "Plasma polymer films and their future prospects", Surf. Coat. Technol., Vol. 125, 371-376 (2000)

[12] Majumder, S. and Bhuiyan, A. H., "DC Conduction Mechanism in Plasma Polymerized Vinylene Carbonate Thin Films Prepared by Glow Discharge Technique", Polymer Science, Ser. A, Vol. 53, 85–91, (2011).

[13] Afroze, T. and Bhuiyan, A. H., "Infrared and ultraviolet-visible spectroscopic studies of plasma polymerized 1, 1, 3, 3-tetramethoxypropane thin films", Thin Solid Films, Vol. 519, 1825–1830, (2011).

[14] Zaman, M. and Bhuiyan, A. H., "Direct current electrical conduction mechanism in plasma polymerized thin films of tetraethylorthosilicate", Thin Solid Films, Vol. 517, 5431-5434, (2009).

[15] Chowdhury, F. U. Z. and Bhuiyan, A. H., "An investigation of the optical properties of the plasma polymerized diphenyl thin films", This Solid Films, Vol. 360, 69-74, (2000).

[16] Chowdhury, F. U. Z and Bhuiyan, A. H., "Dielectric properties of plasma polymerized diphenyl thin films", Thin Solid Films, Vol. 370, 78-84, (2000).

[17] Matin R. and Bhuiyan A. H., "Infrared and ultraviolet-visible spectroscopic analyses of plasma polymerized 2, 6 diethylaniline thin films", Thin Solid Films, Vol. 534, 100–106, (2013).

[18] Akther H. and Bhuiyan A. H., "Dielectric Properties of Plasma Polymerized N,N,3,5 Tetramethylaniline Thin Films", Surf. Rev. Lett., Vol. 18, 53-60, (2011).

[19] Sajeeb, U. S., Mathai C.J., Anantharaman, M.R.," On the optical and electrical properties of rf and ac plasma polymerization aniline thin films" Bull. Matter, Sci., Vol. 29, No.2, pp 159-163, 2006.

[20] Kumar S., D., Kenji N., Nishiyama S., Shigeru I., Hiromichi N., Kunihiro K., and Yasuhiko Y., "Optical and electrical characterization of plasma polymerized pyrrole films" J. App. Phys. Vol. 93 (5), 2705-2711, 2002.

[21] Blaszczyk-Lezak, I., Aparicio, F. J., Borra´s, A., Barranco, A., Alvarez-Herrero, A., Ferna´ndez-Rodrı´guez, M. and Gonza´lez-Elipe, A. R., "Optically Active Luminescent Perylene Thin Films Deposited by Plasma Polymerization", J. Phys. Chem. C, Vol. 113, 431–438, (2009).

[22] Fischer, A. E., McEvoy, T. M. and Long, J. W., "Characterization of ultrathin electroactive films synthesized via the self-limiting electropolymerization of o-methoxyaniline", Electrochimica Acta, Vol. 54, 2962-2970 (2009).

[23] Cherpak, V., Stakhira, P., Hotra, Z., Aksimentyeva, O., Tsizh, B., Volynyuk, D. and Bordun, I., "Vacuum-deposited poly (o-methoxyaniline) thin films: Structure

and electronic properties", J. Non-Crystalline Sol., Vol. 354(35-39), 4282-4286, (2008).

[24] Liang, T., Makita, Y., Kimura, S., „Effect of film thickness on the electrical properties of polyimide thin films", Polymer, Vol. 42, 4867-4872, (2001).

[25] Zhao, X. Y., „Opto-electronic polymer thin films deposited by glow discharge plasma technique: A review", Iran. Polym. J, Vol. 19, (11), 823-841, (2010).

[26] Cho, S. Boo J., „A study on the characteristics of plasma polymer thin film with controlled nitrogen flow rate", Nanoscale Res. Lett., Vol. 7, 62(1-4) (2012).

[27] Cowie, J. M. G., "Polymers: Chemistry and Physics of Modern Materials", Blackie Academic and Professionals, U K, 2nd Ed. (1991).

[28] Ghosh, P., "Polymer Science and Technology of Plastics and Rubbers" Tata McGraw-Hill Pub. Co. Ltd., New Delhi, 4th Ed., (1996).

[29] Lieberman, M. A. and Lichtenberg A. J., "Principles of Plasma Discharges and Materials Processing", John Wiley and Sons, New York, (1994).

[30] Grill, A., "Cold Plasma in Materials Fabrication: From Fundamentals to Applications", IEEE Press, New York, (1994).

[31] Bogaerts, A., Wilken, L., Hoffmann, V., Gijbels, R. and Wetzig K., "Comparison of modeling calculations with experimental result for rf glow discharge optical emission spectroscopy", Spectrochimi. Acta Part B, Vol. 157, 109-119, (2002).

[32] Chu, P. K., Chen, J. Y., Wang, L. P. and Huang, N., "Plasma surface modification of biomaterials", Materials Science & Engineering, R: Reports, R36 (5-6), 143-206, (2002).

[33] Yasuda, H., "Plasma Polymerisation", Academic Press, INC: NY, (1985).

[34] Denes, F., "Synthesis and surface modification by macromolecular plasma chemistry", Trends in Polymer Science (Cambridge, United Kingdom), Vol. 5 (1), 23-31, (1997).

[35] Bogaerts, A. and Neyts, E., "Gas discharge plasma and their applications", Spectrochim. Acta B, Vol. 57, 609-658, (2002).

[36] Chan, C. M., "Polymer Surface Modification and Characterization", Hanser/Gardner Publications, Inc.: Cincinnatti, OH, (1994).

[37] Chan, C. M., Ko, T. M. and Hiraoka, H., "Polymer surface modification by plasmas and photons", Surface Science Reports, Vol. 24 (1/2), 1-54, (1996).

[38] Biederman, H. and Stavinska, D., "Plasma polymer films and their future prospects", Surf. Coat. Technol., Vol. 125(1-3), 371-376, (2000).

[39] Shah Jalal, A. B. M., Ahmed, S., Bhuiyan, A. H. and Ibrahim, M., "On the conduction mechanism in plasma polymerized m-xylene thin films", Thin Solid Films, Vol. 295, 125-130, (1997).

[40] Gibalov, V. I., "Synthesis of ozone in a barrier discharge", Russ. J. Phys. Chem., Vol. 68, 1029-1033, (1994).

[41] Wang, X., Zheng, W.T., Tian, H.W., Yu, S.S., Xu, W., Meng, S.H., He, X.D., Han, J.C., Sun, C.Q. and Tay, B.K. "Growth, structural, and magnetic properties of iron nitride thin films deposited by dc magnetron sputtering", Appl. Surf. Sci., Vol. 220, 30-39, (2003).

[42] Leonhardt, D., Muratore, C., Walton, S.G., Blackwell, D.D., Fernsler, R.F. and Meger, R.A., "Generation of electron-beam produced plasmas and applications to surface modification", Surf. Coat. Technol., Vol. 177-178, 682-687, (2004).

[43] Schlemm, H., Mai, A., Roth, S., Roth, D., Baumgärtner, K.-M. and Muegge, H., "Industrial large scale silicon nitride deposition on photovoltaic cells with linear microwave plasma sources", Surf. Coat. Techno., Vol. 174-175, 208-211, (2003).

[44] Yasuda, H., Vossen, J. L., and Kern, W., "Thin Film Processes", Academic Press, New York, (1978).

[45] Yasuda, H. and Hirotsu, T., "Critical evaluation of conditions of plasma polymerization", J. Polym. Sci., Polym. Chem. Ed., Vol. 16**,** 313-317, (1978).

[46] Yasuda, H. and Lamaze C. E., "Polymerization in an electrode less glow discharge. III. Organic compounds without olefinic double bond", J. Appl. Polym. Sci., Vol. 17, 1533-1544, (1973).

[47] Szycher, M., Sioshansi, P. and Frisch, E. E., Biomaterials for the 1990s: Polyurethanes. Silicones and Ion Beam Modification Techniques (Part II), Spire Corporation, Patriots Park, Bedford, (1990).

[48] Ohl, A. and Schroder, K., "Plasma-induced chemical micropatterning for cell culturing applications: a brief review", Surf. Coatings Technol., Vol. 116-119, 820-830, (1999).

[49] Vargo, T. G., Bekos, E. J., Kim, Y. S., Ranieri, J. P., Bellamkonda, R., Aebischer, P., Margevich, D. E., Thompson, P. M. and Gardella J. A. Jr., "Synthesis and characterization of fluoropolymeric substrate with immobilized minimal peptide sequences for cell adhesion studies. I", J. Biomed. Mater. Res., Vol. 29, 767-778, (1995).

[50] Yasuda, H., Marsh. H. C., Bumgarner, M. O. and Morosoff, N., "Polymerization of organic compounds in an electrodeless glow discharge. VI. Acetylene with unusual comonomers", J. Appl. Polym. Sci., Vol. 19**,** 2845-2858, (1975).

[51] Chakraborti, K., Basu, M., Chaudhuri, S., Pal, A. K. and Hanzawa, H., "Mechanical, electrical and optical properties of a-C : H : N films deposited by plasma CVD technique", Vacuum, Vol. 53, 405-413, (1999).

[52] Nagagawa, K., "Optical anisotropy of polyimide", J. Appl. Polym. Sci., Vol. 41, 2049-2058, (1990).

[53] Davis, E. A. and Mott, N. F., "Conduction in non-crystalline system, Optical absorption and photoconductivity in amorphous semiconductors", Philos. Mag., Vol. 22, 903-922, (1970).

[54] Tauc, J., Menth, A. and Wood, D., "Optical and Magnetic Investigations of the Localized States in Semiconducting Glasses", Phys. Rev. Lett., Vol. 25, 749-752, (1970).

[55] Mott, N. F. and Davis, E. A., "Electronic Processes in Non-Crystalline Materials", Clarendon Press, Oxford, (1971).

[56] Blythe A. R, "Electrical Properties of Polymers" Cambridge University Press, Cambridge (1979) 69-71.

[57] Lamb, D. R., "Electrical Conduction Mechanisms in Thin Insulating Films", Methuen and Co. Ltd., London, (1967).

[58] Shah Jalal, A. B. M., Ahmed, S., Bhuiyan, A. H. and Ibrahim, M., "UV-VIS Absorption Spectroscopic Studies of Plasma-Polymerized M-Xylene Thin-Films", Thin Solid Films, Vol. 288, 108-111, (1996).

[59] Phadke, S. D., Sathianandan, K. and Karekar, R. N., "Electrical conduction in polyferrocene thin films", Thin Solid Films, Vol. 51, 9-11, (1978).

[60] Gould, R. D. and Shafai, T. S., "Conduction in lead phthalocyanine films with aluminim electrodes", Thin Solid Films, Vol. 373 (1-2) (2000) 89-93.

[61] Tolansky, S., "Multiple Beam Interferometry of Surfaces and Films", Clarendon Press, Oxford (1948).

[62] Inagaki, N., "Plasma Surface Modification and Plasma Polymerization", Tehnomic Publishing Co. Inc. UA, (1996).

[63] Morosoff N in: R. d"Agostino (Ed), "Plasma Deposition, Treatment, and Etching of Polymers", Academic Press, San Diego, CA, (1990).

[64] Chowdhury, F-U-Z, Ph. D. Thesis " Preparation and Characterization of Plasma – Polymerized Diphenyl Thin Films", Bangladesh University of Engineering and Technology (BUET), Dhaka, (2000).

[65] Silverstein, R. M., Bassler, G. C., „Spectroscopic Identification of Organic Compounds", John Wiley & Sons, New York, 1981.

[66] Z. Xiongyan H. Xiao, „Preparation and Characterization of Plasma-Polymerized Benzonitrile Films with Ultrafast Optical Kerr Effect" Polym. Engg. Sci., Vol. 40, 2551-2557, (2000).